Pareto Optimal Regulatory Strategies for Coupled Ridesourcing and Taxi Markets with Impatient Passengers

Abstract

This study develops a multi-objective bi-level programming model to identify the Pareto optimal combined regulatory strategy that simultaneously accounts for passengers, taxi drivers, ridesourcing vehicle (RSV) drivers, and the transportation network company (TNC). The upper level determines four regulatory controls, including the RSV fleet cap, taxi fare rate, government-guided RSV fare rate, and TNC wage rate floor, while the lower level obtains steady-state market performance, which is formulated as a fixed-point problem and approximated through iterative agent-based simulations. To solve the model, a multi-objective Bayesian optimization algorithm is developed. Based on the DiDi dataset collected from Hangzhou City in 2018, our experiments demonstrate that no regulatory strategy can simultaneously benefit all stakeholders. If the government considers maximizing vehicle utilization as a secondary criterion, then it should decrease the RSV fleet cap, impose higher fare rates, and allow the TNC to pay lower wages, compared with the benchmark scenario. Furthermore, it is recommended that the government should avoid regulations that primarily favor passengers or the TNC, as our results reveal that such policies could harm other stakeholders and reduce vehicle utilization by up to 11.6%. Finally, if passengers' impatience is overlooked, taxi drivers may lose 23.3% of potential profits.

Keywords

Ridesourcing; Taxi; Impatient Passengers; Order cancellation; Multi-objective Bayesian optimization.

1 Introduction

Ridesourcing services have been growing rapidly in the last few years, driven by the emergence of transportation network companies (TNCs) that offer online platforms to connect passengers and drivers. By facilitating the interaction between passengers and drivers, ridesourcing platforms have reduced the information barrier caused by spatial bias between passengers and traditional taxi drivers. Hence, ridesourcing has been widely acknowledged for its potential to improve urban mobility (Rayle et al., 2016) and to attract a massive number of participants. For example, in China, the number of ride-hailing app users had reached 365 million by December 2020 (Li et al., 2023b). In 2022, Uber reported 131 million monthly active users, with nearly 5.4 million drivers completing 7.64 billion rides worldwide (Campbell, 2023).

However, the proliferation of RSV drivers has led to an oversupply in the ridesourcing market in many regions. This oversupply has contributed to a decline in the traditional taxi industry, prompting taxi drivers to join TNC platforms, which further exacerbates the supply issue. Moreover, the excessive

number of RSVs enables TNCs to reduce wage rates, resulting in a decline in drivers' earnings. Consequently, many RSV and taxi drivers are compelled to work longer hours to meet their daily income targets, thereby creating a vicious cycle that undermines both market stability and transportation efficiency. Such a vicious cycle highlights the necessity of government regulation for coupled ridesourcing and taxi market (CRTM). The objective of this study is therefore to identify optimal regulatory strategies accommodating the interests of different stakeholders in CRTM.

The existing literature and practice have identified four main types of regulatory strategies, each aiming to improve welfare for specific stakeholders: i) Control the number of RSVs. In China, many city governments have capped the number of RSVs (Yu et al., 2020; Yang et al., 2021; Zhong et al., 2022). ii) Regulate taxi fares (Yu et al., 2020; Zhong et al., 2022). iii) Set RSV prices (Yang et al., 2021; Chen et al., 2024). TNCs in China are required to follow the government-guided fare rates when necessary. iv) Set the minimum wage paid by TNCs to drivers (Zha et al., 2018a; Ke et al., 2021; Vignon et al., 2023). In 2018, the New York City Council required that TNCs pay drivers a minimum wage (Shapiro, 2018).

Nevertheless, each strategy could potentially favor certain stakeholders and negatively impact other stakeholders. For example, limiting fleet size can increase the average profits of both RSV and taxi drivers, but it could lead to longer waiting times and potentially higher trip fares for passengers. In most existing ridesourcing studies, the overall impact of regulatory strategies on various stakeholders is typically modeled as a single objective, namely the social welfare (Yu et al., 2020; Tang et al., 2023; Mo et al., 2024). In contrast, this study aims to fill the gap to optimize regulatory strategies from a multi-objective Pareto optimal perspective. Meanwhile, to the best of our knowledge, no existing study has examined whether implementing a combination of these four regulatory strategies would be more effective than applying them individually, or, if so, how to optimize such strategies. It is important to fill this gap because fragmented regulation can skew the distribution of benefits in the market and may even result in substantial losses for certain stakeholders.

Essentially, regulatory strategies shape the market by influencing the behavior of drivers and passengers, such as drivers' work decisions and passengers' travel choices. This underpins the rationale for developing a bi-level programming model, where the upper level determines regulatory strategies, while the behavioral dynamics or interactions between market supply and demand can be captured in the lower-level model, and a steady-state market performance can be obtained by solving it. Notably, a distinct feature of the CRTM market is the impact of passenger impatience on overall performance. This impact can be observed in two main forms.

1) Passengers may cancel orders after sending online travel requests, not only due to incorrect entries or sudden changes in plans but also as a result of long waiting time or encountering vacant taxis (He et al., 2018). Cancellation behaviors caused by vacant taxis differ before and after order matching (Xu et al., 2022). Post-matching cancellations waste the limited supply and prevent other passengers from accessing potential travel opportunities (Wang et al., 2020), which is why passengers are usually charged a penalty in practice. In contrast, pre-matching cancellations reduce TNC profits but typically

do not impose additional costs on passengers or harm market efficiency; in some cases, they may redirect demand toward taxi services, thereby supporting taxi drivers' earnings.

2) Passengers may update their requested hailing types between RSV and taxi services. For example, if an RSV passenger experiences prolonged waiting without a successful match, they may request taxi services due to impatience. This behavior is supported by certain ride-hailing apps, e.g., DiDi, which allows passengers to append new service types within the same platform before matching.

The above impatient behaviours of passengers and their dynamic order matching with drivers are shaped by the short-term market environment, which, inherently, is the consequence of government regulatory strategies. Moreover, these behaviors could also endogenously impact market supply and demand in the long term, which in turn could lead to different behavioral patterns of passengers and drivers. To capture this feedback loop, we formulate a fixed-point problem to characterize the steady-state market performance under a given regulatory strategy. Then, we develop an agent-based simulation to depict the microscopic behaviors and capture their endogenous interactions. The steady-state market performance is approximated by averaging the results from iterative simulations. This simulation framework, mapping the complex nonlinear correlations of regulatory inputs to steady-state performance outputs, can be treated as a black-box function. Therefore, to efficiently solve for the optimal combined regulatory strategy within this black-box system, we utilize the multi-objective Bayesian optimization algorithm.

To sum up, this study aims to determine the optimal combinatorial configuration of four existing regulatory strategies on CRTM, considering the endogenous interaction between supply and demand with impatient passengers.

The main contributions of this study are summarized as follows:

(1) We formulate a bi-level multi-objective model for regulating CRTM. In contrast to prevailing single-objective studies that focus on designing one or two regulatory instruments, this study simultaneously optimises four prevalent regulatory strategies with the aim of maximising the benefits of passengers, taxi and RSV drivers, and the TNC.

(2) We develop a comprehensive agent-based simulation model that advances existing ridesourcing studies by capturing more realistic behavioural dynamics, including passengers' travel mode and hailing type choices, impatient passengers' abandonment and cancellation behaviors before and after order matching, and taxi drivers' work decisions between hybrid and street modes.

(3) We develop a solution methodology based on multi-objective Bayesian optimization. The objective functions are evaluated under the steady-state market performance, which is formulated as a fixed-point problem and approximated using iterative agent-based simulations. This framework can also be applied to other ridesourcing studies.

(4) We contribute several regulatory insights for the government from a Pareto optimal perspective. In brief, it recommends fewer RSVs, higher fare rates, and lower RSV wage rates, and the government should avoid prioritizing passengers or the TNC. Meanwhile, making passengers bear more costs appears to be an unavoidable sacrifice to improve overall market performance. Also, taxi

drivers may lose potential profits while ignoring passengers' impatience.

The remainder of this paper is organized as follows. Section 2 reviews the relevant literature. Section 3 defines the problem statement and formulates the bi-level programming model. Section 4 develops an agent-based simulation and outlines the solution framework. Section 5 conducts numerical experiments to validate the model, evaluate the impact of regulatory strategies, and identify Pareto optimal combined regulatory strategies. Finally, Section 6 concludes the main findings of this study and highlights directions for future research.

2 Literature review

This study is situated at the intersection of three key research streams: the regulation of ridesourcing services, modelling approaches for ride-hailing markets, and the optimization of black-box bi-level problems.

2.1 Regulation for ridesourcing services

In recent years, regulatory strategies for ridesourcing services have attracted growing attention (Zha et al., 2016; Zha et al., 2018a; Li et al., 2019). To enhance social welfare, typical regulatory strategies include limiting the number of vehicles, controlling the fare rates of ridesourcing and taxi services, and guaranteeing drivers' wage floors. Yu et al. (2020) showed that lowering taxi fare rates can improve overall social welfare. Yang et al. (2021) found that under fare rate regulation, TNCs would charge higher fares. Zhong et al. (2022) discovered that regulating the rates and number of taxis and RSVs can effectively increase social benefits. Vignon et al. (2023) showed that the government can maximize social surplus by regulating TNCs' per-trip commission (i.e., the difference of fare and driver earning per ride).

Other than improving the social welfare, alternative perspectives have been introduced to regulate the ridesourcing market. Qin et al. (2025) investigated whether the government could use a price-cap regulation and subsidy policy to encourage the ridesourcing platform to serve as a complement to public transit services. They found that the platform's profit decreased as the price-cap decreased and increased with the size of the subsidy, and under certain supply-demand ratios, both strategies could increase public transit ridership. Mo et al. (2024) studied how governments can regulate the ridesourcing market integrated with vehicle rental services through minimum driver wages and maximum vehicle rental fees. They found that when the government focused on only one policy without coordinating with the other, not all groups benefited; however, when the two policies are coordinated, higher total social welfare could be achieved.

It is worth noting that most of the preceding literature only considers a single objective. Few studies have investigated the impact of regulatory strategies from a multi-objective perspective. Ke et al. (2021) studied the effects of various regulatory strategies for the ridesourcing market from a Pareto-efficient perspective, considering traffic congestion and drivers' heterogeneity. In their study, the Pareto frontier is defined by the platform's profit and social welfare, where the social welfare is

modeled as a linear sum of platform profit, passenger surplus, and other elements. However, their Pareto frontier does not fully capture the perspectives of all stakeholders, namely, passengers, taxi drivers, RSV drivers, and the TNC.

2.2 Ridesourcing and taxi market modeling

Early research on modeling the ridesourcing and taxi market primarily relied on steady-state market equilibrium analyses, employing economic models to characterize driver-passenger interactions and passengers' travel choices. (e.g., Yang et al., 2010; He and Shen, 2015; Wang et al., 2016; Zha et al., 2018b; Wang et al., 2020; Karamanis et al., 2021). Within this modeling approach, the existence of market equilibrium can be proved, and the effects of factors such as pricing and fleet size on the market have been examined. It is generally acknowledged that raising prices increases passengers' travel costs, thus leading to lower demand (Wang et al., 2016; Ke et al., 2020), while increasing fleet size makes the operation less efficient and less profitable for drivers (Liu et al., 2022a).

However, early studies overlooked a critical issue: not all ridesourcing requests can be completed, as a substantial proportion are canceled by passengers, which has a significant impact on the on-demand service platforms (Xu et al., 2021a). A primary reason that passengers cancel their requests is encountering vacant taxis. With the data collected by DiDi in Shanghai, Wang et al. (2020) illustrated the effect of vacant taxis on passengers' cancellations toward confirmed orders from a macro perspective. They calibrated a nonlinear aggregation model to characterize this effect. Furthermore, passengers' cancellations before and after order matching could be different (Ramezani and Valadkhani, 2023). Jiao and Ramezani (2022) defined two types of cancellations in ridesourcing services: pre-matching abandonment, where passengers withdraw their request due to impatience before being matched; and post-matching cancellation, where passengers cancel confirmed orders due to dissatisfaction with the provided waiting time and trip fare. Many recent studies that consider passengers canceling ridesourcing services have taken into account different cancellations before and after order matching (Jiao and Ramezani, 2024; Wang et al., 2024; Jiao and Ramezani, 2025; Liu et al., 2025). In these studies, pre-order-matching cancellations are usually modeled as passengers abandoning their requests after reaching a maximum waiting time threshold, while post-order-matching cancellations are usually modeled based on the utility difference between ridesourcing and other travel services. For CRTM, passengers may encounter vacant taxis not only after order matching but also before, and they may also cancel their online orders before order matching (Xu et al., 2022). However, such pre-order-matching cancellations are different from abandonment because, although the TNC loses the same profit, the passenger's hailing demand is satisfied.

It should be noted that both RSVs and taxis can provide hailing services in CRTM, allowing passengers to choose between these two options. Existing CRTM studies generally assume that hailing demand is segmented into ridesourcing and taxi passengers (Wang et al., 2020; Xu et al., 2022). However, in real-world scenarios, passengers may simultaneously request both services. Furthermore, for impatient passengers, the sunk waiting cost may influence their decision-making behavior before

matching (Liu et al., 2024b). However, to the best of our knowledge, no existing study has investigated passengers' dynamic updating of hailing types while awaiting a match.

In recent years, scholars have increasingly recognized the limitations of the traditional steady-state equilibrium-based modeling approach due to the complexity of the ridesourcing market. While previous studies have proven the existence of a market equilibrium state (Yang et al., 2010; Wang et al., 2016), such an equilibrium state is highly idealized and seldom observed in real-world markets, where supply and demand fluctuate continuously (Nie, 2017; Hamedmoghadam et al., 2019). When operational decisions in the market significantly change the state of the system, it takes a long time to restore the equilibrium state, which limits the applicability of economic models in practice (Nourinejad and Ramezani, 2020). Meanwhile, many traditional models assume that vehicles are parked when waiting for matching (Wang et al., 2020; Xu et al., 2022), making it challenging to describe the complex interaction between passengers and drivers in the real world and to accurately identify some key metrics, e.g., passengers' waiting time and vehicle utilization.

Consequently, researchers have increasingly turned to agent-based modeling to construct dynamic interactions between drivers and passengers (Wen et al., 2018; Beojone and Geroliminis, 2021; Cheong et al., 2023; Feng et al., 2023; Yao and Bekhor, 2024). In addition, agent-based modeling offers greater flexibility in representing taxi drivers' work mode choices, thereby facilitating the design of new operational mechanisms (Martinez et al., 2015). Therefore, this study develops an agent-based simulation model for the CRTM. Table 1 compares the modeling methods used in this study with those used in the literature. As summarized in the table, our model comprehensively accounts for passengers' pre-order matching abandonments and cancellations before and after order matching, and it also models the travel mode and hailing type choices of passengers, as well as the work mode choices of taxi drivers.

Table 1

Comparison with existing methods of the ridesourcing market modeling.

Literature	Passenger's behaviors					Driver's behaviors		System characteristics	
	Abandonment	Cancel before order matching	Cancel after order matching	Travel mode choice	Hailing type choice	Taxi work mode choice	Move while idling	Coupled RSV & taxi market	Dynamic supply and demand
Aggregation model									
Wang et al. (2016)							√	√	
He et al. (2018)			√	√		√	√	√	
Wang et al. (2020)			√		√			√	
Xu et al. (2022)		√	√		√			√	√
Queue model									
Banerjee et al. (2015)	√								
Sun et al. (2020)						√			
Feng et al. (2021)									√
Feng et al. (2022)	√								
Simulation model									
Agatz et al. (2011)							√		√
Nourinejad and Ramezani (2020)							√		√
Beojone and Geroliminis (2021)	√			√			√	√	√
Yao and Bekhor (2024)		√	√				√		√
Our research	√	√	√	√	√	√	√	√	√

Table 1 shows that there is still a gap in the literature regarding constructing a comprehensive simulation model of the CRTM that explicitly considers the actions of drivers and passengers during the hailing service.

2.3 Bayesian optimization in solving black-box bi-level problems

In a general bi-level model for solving a transportation problem, the upper-level model determines the decisions of leaders, such as the government and operator, with the aim of maximizing or minimizing their objectives while considering the responses of the lower-level followers (Clegg et al., 2001; Santos et al., 2021), which be formulated either as analytical models that are solved by exact or approximate solutions (e.g., Ni et al., 2021; Xu et al., 2021b) or simulation models that can be treated as a black-box (Zhong et al., 2021; Huo et al., 2023a; Gong et al., 2025).

Bayesian optimization is a gradient-free optimization method that typically uses the Gaussian process regression as a probabilistic surrogate model to construct the analytical function for the black-box problem. The Gaussian process regression is more flexible than linear regression models because it does not assume a functional form for the mapping from input to output. As a result, it can capture complex and highly nonlinear relationships based on fewer sample points (Liu et al., 2022b). Other gradient-free methods, such as the genetic algorithm (Wei and Sun, 2018) and particle swarm optimization algorithms (Han et al., 2016), are also widely used in bi-level programming problems. In comparison, Bayesian optimization reduces the need for repeated evaluations of the lower-level model, resulting in greater computational efficiency and yielding higher-quality solutions (Olofsson et al., 2018).

Existing research has demonstrated the effectiveness of Bayesian optimization in solving black-box and bi-level problems (Zhong et al., 2021; Huo et al., 2023b). Yang et al. (2023) employed Bayesian optimization to jointly design the fleet size and charging facility configuration of an electric automated on-demand mobility system. Their results show that the method can find satisfactory solutions within a tight computational budget. Huo et al. (2023a) demonstrated that Bayesian optimization outperforms the simultaneous perturbation stochastic approximation method and the method proposed by Osorio (2019) in terms of solution efficiency and estimation accuracy when solving a bi-level OD estimation problem. Liu et al. (2024a) developed a multi-objective bi-level programming model to solve the joint optimal pricing problem of shared autonomous vehicles and road congestion pricing. They obtained an optimal solution that can simultaneously improve regional accessibility and transportation efficiency with the help of Bayesian optimization.

3 Problem statement

We consider a CRTM with a single TNC operating in a specific period and urban area, where both RSVs and taxis can provide hailing services. The fleet size of RSVs is fully controlled by the TNC, while the size of taxis is fixed and determined by the government. Taxis can serve roadside passengers through traditional cruising or accept assignments from the TNC to serve online orders (Wang et al., 2016; He et al., 2018). If a taxi is unwilling to accept online assignments during the study period, it is defined as a ‘street’ taxi, which only searches for roadside passengers by cruising; otherwise, if it is willing to accept online assignments, it is defined as a ‘hybrid’ taxi, which can also serve roadside passengers when idle. Hybrid taxis receive full fare payments from passengers when operating in

cruising mode, similar to traditional street-hailing taxis. When accepting online assignments from the TNC, they earn a portion of the passenger payments as wages, like RSV drivers. Both taxi and RSV drivers bear vehicle fuel and operation costs themselves. Passengers can choose between hailing services and public transit to meet their travel needs. Passenger impatience manifests in three ways: 1) abandonment of requests due to excessive waiting time before order matching, 2) cancellation of unmatched or matched requests upon encountering vacant taxis either before or after the order matching, and 3) updating their hailing type while waiting to be matched. The TNC generates income by offering ridesourcing and online taxi services to passengers and incurs costs through wage payments to RSV and hybrid taxi drivers.

In the online hailing process, passengers first send their travel requests along with their preferred hailing type(s) to the TNC. Then, the TNC matches passengers with available hailing vehicles (i.e., RSVs and hybrid taxis) corresponding to their hailing requests. Once matched, the assigned vehicle moves to pick up the passenger. If the passenger continues to wait till the vehicle arrives without canceling, the driver collects the passenger and transports them to the requested destination.

In such a market, the government could intervene through four regulatory instruments: 1) capping the number of RSVs, Z^{rsv}, 2) setting a regulated fare for taxi services, α^{taxi}, 3) imposing a government-guided RSV fare rate, α^{rsv}, and 4) establishing a regulatory floor on the wage paid by the TNC to RSV drivers, τ^{rsv}. The combination of these four is termed a combined regulatory strategy $\boldsymbol{\varphi} = [Z^{\text{rsv}}, \alpha^{\text{taxi}}, \alpha^{\text{rsv}}, \tau^{\text{rsv}}]$. In response to a combined regulatory strategy, the TNC determines the number of operating RSVs and the wage rate for RSV drivers to maximize its profit while complying with the government-guided RSV fare rate. Meanwhile, taxi drivers would make a work mode choice between providing online and traditional services, and passengers may act to make various travel decisions. As a result of the combined regulatory strategy and the responses from the CRTM, the system results in different performance measurements, including the average hailing cost of passengers $\bar{C}$, the average profit of taxi drivers, Q^{taxi}, the average profit of RSV drivers, Q^{rsv}, and the profit of the TNC, Q^{TNC}. The four indicators serve as proxies for the welfare (objectives) of passengers, taxi drivers, RSV drivers, and the TNC, respectively.

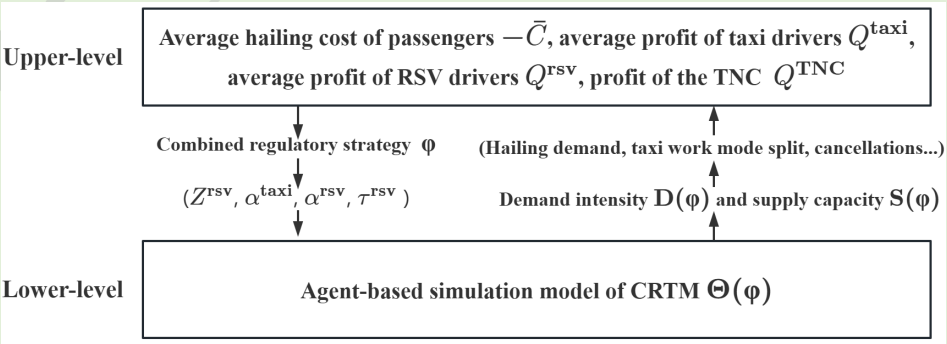

Fig. 1. The framework of the multi-objective bi-level programming model

Under the preceding setting, this study aims to determine an optimal combined regulatory strategy to cater to the interests of four stakeholders simultaneously and to identify the Pareto frontier to support

government decision-making. To this end, we adopt a bi-level programming approach. As illustrated in Fig. 1, the upper level aims to find a combined regulatory strategy, $\boldsymbol{\varphi}$, that leads to a Pareto optimal solution in four objectives, where $\bar{C}$ is associated with a negative sign to reflect cost minimization. The lower level is a simulation model that captures the supply-demand interaction and computes the objective functions under the combined regulatory strategy $\boldsymbol{\varphi}$ to obtain stabilized market performance.

The following multi-objective bi-level programming model is formulated.

$$\max_{\boldsymbol{\varphi}} \mathbf{f}\left(\boldsymbol{\varphi}, \mathbf{D}(\boldsymbol{\varphi}), \mathbf{S}(\boldsymbol{\varphi})\right), \tag{1}$$

s.t.

$$\boldsymbol{\varphi} \in \Omega, \tag{2}$$

$$\mathbf{f}\left(\boldsymbol{\varphi}, \mathbf{D}(\boldsymbol{\varphi}), \mathbf{S}(\boldsymbol{\varphi})\right) = \left\{ f^{\omega}\left(\boldsymbol{\varphi}, \mathbf{D}(\boldsymbol{\varphi}), \mathbf{S}(\boldsymbol{\varphi})\right),\ \omega = 1,2,3,4 \right\}, \tag{3}$$

$$\left[\mathbf{D}(\boldsymbol{\varphi}), \mathbf{S}(\boldsymbol{\varphi})\right] = \Theta(\boldsymbol{\varphi}). \tag{4}$$

$\mathbf{f}(\cdot)$ denotes the vector of the four objective functions, where f^{ω} is the ω^{th} objective function. Ω is the solution space of the regulatory strategies. $\mathbf{D}(\boldsymbol{\varphi})$ and $\mathbf{S}(\boldsymbol{\varphi})$ represent the stable demand level and supply capacity under $\boldsymbol{\varphi}$. $\Theta(\boldsymbol{\varphi})$ denotes the lower-level agent-based simulation model of CRTM, reflecting the market performance under the combined regulatory strategy $\boldsymbol{\varphi}$. Eq. (3) states that $\mathbf{f}(\cdot)$ consists of four objective functions, each of which is measured by the same $\boldsymbol{\varphi}$ and corresponding stable market supply and demand. Eq. (4) represents that the stable market supply and demand are obtained from the lower-level model.

Solving the above bi-level model is challenging because the relationship between decision variables and objective functions is complex and nearly black-box. The following Fig. 2 shows the effects and interactions in the research problem and the composition of each objective function. The gradient-colored boxes in the left and right parts of Fig. 2 represent the decision variables and objective functions, respectively. The white and gray boxes in the center represent endogenous and exogenous variables, respectively. The blue arrow represents a positive effect between a pair of components, while the red dashed arrow represents a negative effect. Decision variables and exogenous variables could have positive or negative effects on different endogenous variables. Essentially, by influencing the supply-demand pattern, decision variables can have a complex impact on objective functions. Note that the endogenous/exogenous variables involved in this figure and the effects between variables are not exhaustive, but they can reflect the basic mechanism of how the combined regulatory strategy influences CRTM.

To effectively model the sophisticated interactions, an agent-based simulation is developed to characterize the complex influence process and identify the steady-state market performance of CRTM

under different combined regulatory strategies. To solve the model, a solution methodology based on multi-objective Bayesian optimization is developed. In what follows, we first introduce the key definitions, assumptions, and notations for the model, and we leave the notation for the multi-objective Bayesian optimization theory to be explained at usage in Section 4.4.

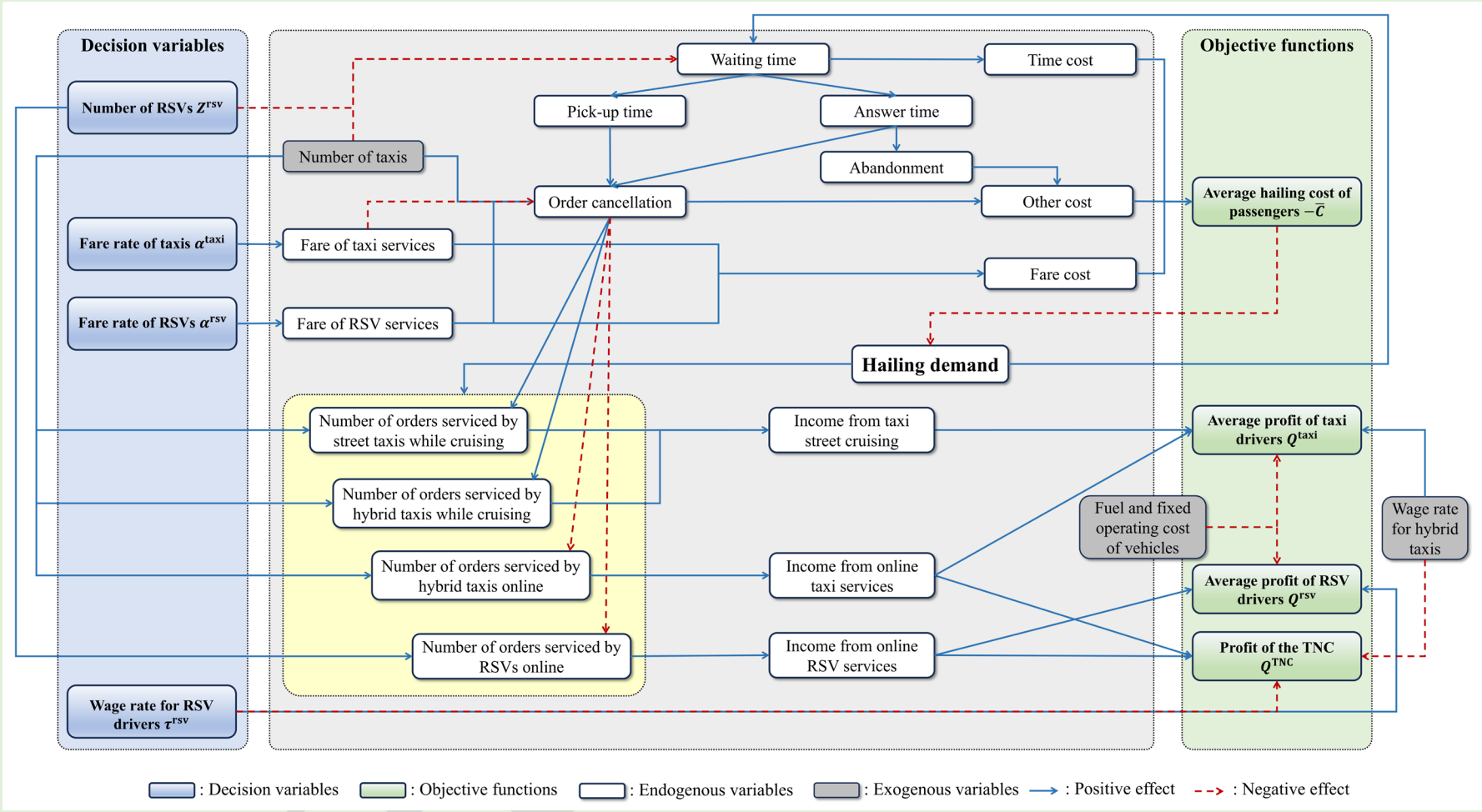

Fig. 2. The effects and interactions in the research problem

The following definitions clarify several "rates" with different meanings and units in this study.

Definitions 1. Fare rate (¥/km): the fare charged from passengers per kilometer for taking ridesourcing or taxi services.

Definitions 2. Wage rate (%): the percentage of fare income (charged from passengers) paid by the TNC to the assigned RSV or hybrid taxi driver for each completed online service.

Definitions 3. Demand rate (requests/min): the number of travel demands per minute.

The following assumptions clarify some basic supply-side settings in the model.

Assumption 1. Existing literature generally assumes that the number (or working hours) of drivers who provide hailing services is positively correlated with the expected profit (Nourinejad and Ramezani, 2020; Wang et al., 2020; Xu et al., 2022). However, in the real world, drivers are more likely to extend their working hours to reach their daily profit targets when their average profit declines, and they also tend to reduce break time after facing cancellations (Duong et al., 2023). Therefore, this study assumes that the number of taxis is exogenous and fixed during the study period. The same assumption has been adopted by Yu et al. (2020) and Zhong et al. (2022).

Assumption 2. Without loss of generality, it is assumed that there will always be some street taxis in the market that seek roadside passengers by cruising. In practice, experienced taxi drivers often take the opportunity to operate efficiently by declining online orders that require more idle miles and time in specific areas or periods, such as busy shopping areas or peak commuting hours.

Assumption 3. The wage rate for taxi drivers in our model is assumed to be exogenously given. This reflects the fact that taxi fare rates are regulated by the government rather than decided by the TNC, thereby requiring the TNC to pay hybrid taxi drivers a regulated and fixed wage rate.

Assumption 4. Once an order is matched, the assigned RSV or hybrid taxi driver is not allowed to cancel the order. This is a reasonable simplification since TNCs impose very strict rules and penalties on driver-side cancellation in practice. For example, DiDi drivers are only allowed to cancel under limited circumstances, but cannot cancel more than 3 times a day. If a driver cancels frequently, the TNC would reduce the driver's future matching probability or impose temporary suspensions.

Table 2

Notations.

Symbol	Description
Sets	
$\boldsymbol{\varphi}$	Set of a combined regulatory strategy
$\mathbf{f}$	Set of objective values
G^{rsv}, $G^{\text{h-taxi}}$	Set of passengers who are served by RSVs or hybrid taxis online, respectively
G_{cancel}	Set of passengers who cancel their orders before order matching

$G_{\text{cancel}}^{\text{rsv}}$, $G_{\text{cancel}}^{\text{h-taxi}}$	Set of passengers who cancel RSV or hybrid taxi orders after order matching, respectively
G_{abandon}	Set of passengers who abandon their requests before order matching
$G_{\text{street}}^{\text{h-taxi}}$, $G^{\text{s-taxi}}$	Set of passengers who are served by hybrid taxis or street by traditional cruising, respectively
$\boldsymbol{\varphi}^*$	Set of the Pareto optimal output solution
Decision variables	
Z^{rsv}	Number of RSVs (veh)
α^{taxi}	Fare rate of taxis (¥/km)
α^{rsv}	Fare rate of RSVs (¥/km)
τ^{rsv}	Wage rate paid by the TNC to RSV drivers (%)
Objective functions	
$\overline{C}$	Average hailing cost of passengers (¥)
Q^{taxi}	Average profit of taxi drivers (¥)
Q^{rsv}	Average profit of RSV drivers (¥)
Q^{TNC}	Profit of the TNC (¥)
Endogenous variables	
λ, λ^{transit}	Hailing demand rate and public transit demand rate (requests/min)
$U_i^s(t), s \in \{\text{rsv,taxi}\}$	Passenger *i*'s mental accounting utility for hailing type *s* after his/her order is initiated *t* minutes (¥)
$\hat{u}_i$	Passenger *i*'s valuation for unit travel distance (¥/km)
$u_i(t)$	Passenger *i*'s mental account value for unit travel distance after his/her order is initiated *t* minutes (¥/km)
W_i^{answer}, W_i^{pick}	Passenger *i*'s order answer time and pick-up time, respectively (min)
$W_i^{\text{b-vacant}}$, $W_i^{\text{a-vacant}}$	Passenger *i*'s waiting time to encounter a vacant taxi before and after order matching, respectively (min)
C_i^1, C_i^2	Utilities associated with keeping waiting and canceling an order upon passenger *i* encountering a vacant taxi after order matching, respectively (¥)
$N(T,\lambda)$	The number of passengers who arrived and ended hailing service at the hailing demand rate λ during a time interval T
C_i	Passenger *i*'s generalized hailing cost (¥)
$\overline{L}$	The logsum of the disutility as perceived by a passenger choosing hailing services to meet travel demand (¥)
$\overline{C}^{\text{rsv}}$, $\overline{C}^{\text{taxi}}$	The average travel costs of passengers served by RSVs and taxis, respectively (¥)
$Z^{\text{h-taxi}}$, $Z^{\text{s-taxi}}$	Number of hybrid and street taxis, respectively (veh)
$Q^{\text{h-taxi}}$, $Q^{\text{s-taxi}}$	Average profits of hybrid and street taxi drivers, respectively (¥)
β^{rsv}, $\beta^{\text{h-taxi}}$	Time cost coefficient of RSVs and hybrid taxis, respectively (¥/min)

$\bar{L}(\boldsymbol{\varphi},\lambda)$	The logsum disutility of hailing passengers under λ and $\boldsymbol{\varphi}$ (¥)
$\lambda^*(\boldsymbol{\varphi})$	The endogenously stable hailing demand rate under $\boldsymbol{\varphi}$ (requests/min)
Parameters / Exogenous variables	
T	The duration of a single time interval (min)
M	The scale of the grid-type road network
l_i	Travel distance for passenger *i* (km)
$\bar{l}$	Average travel distance of all passengers (km)
R	The maximum matching distance (km)
Λ	Total travel demand rate (requests/min)
$u_{\max}$	Passengers' highest hailing value rate (¥/km)
$\bar{C}^{\text{transit}}$	Average public transit cost (¥)
$\bar{W}^{\text{tansit}}$	Average waiting time for public transit service (min)
α^{transit}	Fare rate of public transit (¥/km)
Z^{taxi}	Number of taxis (veh)
τ^{taxi}	Wage rate paid by the TNC to hybrid taxi drivers (%)
$W_{\max}$	Maximum patience time of passengers (min)
$\beta_{\text{time}}^{\text{pas}}$	Time cost coefficient of passengers (¥/min)
$\beta_{\text{sunk}}^{\text{pas}}$	Sunk time cost coefficient of passengers (¥/km·min)
$\hat{p}$	Penalty for canceling a matched order (¥)
H	The psychological cost of canceling a matched order (¥)
v, v^{tansit}	The average speed of hailing vehicles and transit vehicles, respectively (km/min)
γ	Fuel cost per unit distance of hailing vehicles (¥/km)
$\hat{\gamma}^{\text{rsv}}$, $\hat{\gamma}^{\text{taxi}}$	Fixed operating cost of RSVs and taxis at each time interval, respectively (¥)
θ^{pas}, θ^{taxi}	Dispersion coefficients used in the Logit model
θ_0	The logsum parameter
Ω	Solution space of decision variables

Note: 1¥≈0.15US$.

4 Methodology

4.1 Agent-based simulation

This study examines a CRTM with three main types of agents (i.e., passengers, RSVs, and taxis) in a grid-type road network (Fig. 3) following the prevailing studies (e.g., Feng et al., 2021; Besbes et al., 2022; Wang et al., 2024). The horizontal and vertical lines in the figure represent bidirectional roads for RSVs and taxis to travel. Our simulation model is inspired by Feng et al. (2021) and inherits a similar setting, in which the spatial heterogeneity of the road network is not considered, and the impact of private vehicles on traffic is reflected through average speed. The details of agents' states, behaviors,

properties, and KPIs are summarized in Appendix A.

The simulation is time-based, and its runtime horizon consists of multiple time intervals, the length of each time interval is T minutes, and each minute indicates a time stamp. During each time interval, the CRTM's operational configuration is fixed, including the fleet sizes, fare rates, and wage rates paid by the TNC to drivers, and it is assumed that the travel demand remains unchanging. As for passengers, they enter the system following a Poisson process with a given total travel demand rate, Λ. Their origins and requested travel destinations are randomly generated at intersections of the horizontal and vertical lines. Denote passenger i's initial location and destination are (x_i, y_i) and (x_i', y_i'), respectively. His/her travel distance can be expressed in terms of a Manhattan Distance as follows,

$$l_i = \left\| (x_i' - x_i, y_i' - y_i) \right\|_1 . \tag{5}$$

Considering an $M * M$ grid road network, the average travel distance of passengers is

$$\bar{l} = \frac{2\left(M^2 - 1\right)}{3M} . \tag{6}$$

For RSVs and taxis, their starting positions are randomly located in the road network, and their current travel directions are randomly set based on their locations. In the agent-based simulation, all vehicles remain in motion and do not park. When the time stamp updates, all vehicles move toward their current travel directions at a fixed travel speed v, after which they update their new travel directions based on their new locations and service states, i.e., idle, picking up, or in-service. Vehicles in picking-up and in-service states update their direction and trajectories according to the shortest path to the matched passengers and their requested destinations. Idle vehicles may choose any available direction except the one opposite to their current heading.

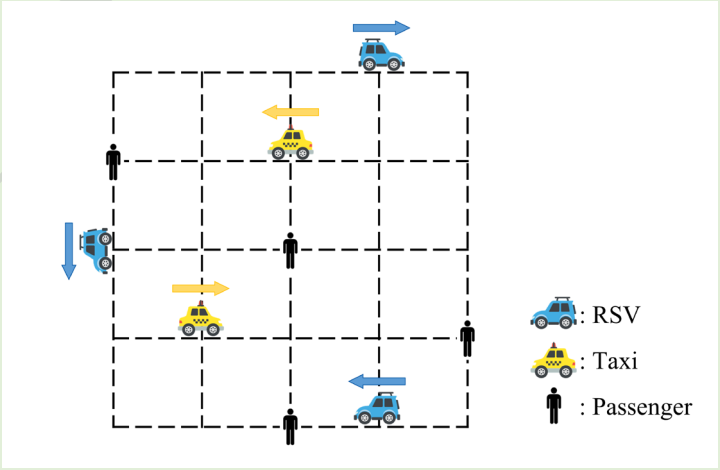

Fig. 3. Example of a grid-type road network

The TNC receives passengers' requests and matches them with RSVs and hybrid taxis. For the

matching strategy, we employ the well-known Nearest Neighbor (NN) scheduling algorithm (Bertsimas and Van Ryzin, 1991). When a passenger arrives, if there are vehicles available in the system, he/she will be matched with the closest one. If there is no available vehicle, he/she will wait until there is an available one, and he/she is also the earliest arriving and closest passenger to the vehicle among all waiting passengers. It is also important to note that any pair of matches must be within the maximum matching distance R to avoid long waiting times for passengers and a 'wild goose chase' for long pick-up distances of vehicles.

The activities and interactions of passengers, RSVs, and taxis are illustrated in Fig. 4. Once passengers enter the system with an arrival rate of Λ, they first choose a travel mode between hailing service and public transit. The latter, as an alternative to hailing services, has a lower fare rate α^{transit}, slower travel speed v^{tansit}, but longer average waiting time $\bar{W}^{\text{tansit}}$. In this paper, we employ the Logit model to approximate the split between the two travel modes (He et al., 2018; Li et al., 2022), with details provided in Section 4.2. The resultant demand rates for hailing and public transit are given by λ and λ^{transit}, respectively, and $\lambda + \lambda^{\text{transit}} = \Lambda$.

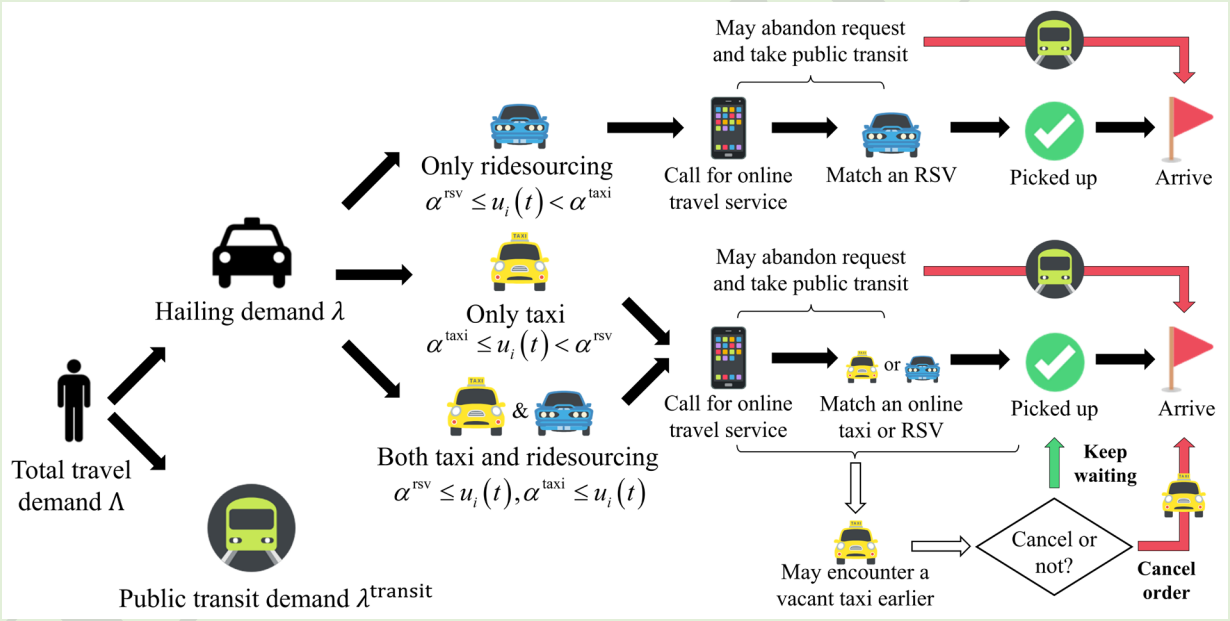

Fig. 4. Passenger's choice process of travel model and hailing type

For passengers selecting hailing services, their subsequent decision concerns which type of hailing vehicles to request. Following Banerjee et al. (2015), Bai et al. (2019), and Yu et al. (2020), this study proposes a method that selects the option(s) with the positive utility of hailing service. This utility comprises the fare cost and the passenger's valuation associated with his/her trip. Meanwhile, we assume that the sunk cost due to wasted waiting time influences the hailing type decisions of impatient passengers.

In line with Ülkü et al. (2020), we introduce the concept of mental accounting to characterize passengers' impatient behavior while waiting to be matched. According to Thaler (1980, 1985, 1990,

1999), people tend to record the time, money, or effort they have already invested in a virtual 'mental account' and do not immediately perceive these as a loss. When making decisions, to avoid a 'deficit' in the 'mental account,' people tend to 'offset' previous investments by increasing consumption, thereby demonstrating the sunk-cost effect. In this study, we consider that the sunk-cost effect on passengers caused by the elapsed waiting time would motivate them to request more hailing types before order matching. Meanwhile, it is assumed that this sunk-cost effect becomes more pronounced as the potential trip distance increases (Liu et al., 2024b).

To model such an impatient behavior, the mental accounting utility is adopted, which consists of the passenger's valuation on the trip, the fare cost of the trip, and the sunk cost utility. Specifically, the valuation represents the monetary value of the requested trip to the passenger, which may vary depending on the purpose and distance of the trip. For passenger *i*, the mental accounting utility regarding hailing type $s \in \{\text{rsv},\text{taxi}\}$ at elapsed waiting time *t* can be formulated as

$$U_i^s(t) = \hat{u}_i \cdot l_i - \alpha^s \cdot l_i + \beta_{\text{sunk}}^{\text{pas}} \cdot l_i \cdot t, \tag{7}$$

where the first term on the right side of Eq. (7) represents the trip valuation, in which $\hat{u}_i$ denotes passenger *i*'s valuation for unit trip distance; the second term represents the fare cost, where α^s denotes the fare rate of hailing type *s*; the third term defines the sunk cost utility, and the coefficient $\beta_{\text{sunk}}^{\text{pas}} \geq 0$ represents the effect of sunk waiting time on the passenger's decision. In this study, we assume that passenger *i* is willing to request the corresponding hailing type *s* only if $U_i^s(t) \geq 0$.

Subsequently, define $u_i(t) = \hat{u}_i + \beta_{\text{sunk}}^{\text{pas}} \cdot t$, it denotes passenger *i*'s mental account value for unit trip distance at *t*, then $U_i^s(t) \geq 0$ can be reduced to $u_i(t) \geq \alpha^s$ by canceling l_i. This means that if $u_i(t)$ is higher than the fare rate of a particular hailing service, α^{rsv} or α^{taxi}, then passenger *i*'s mental accounting utility is positive at *t* and would choose the corresponding hailing type *s*, i.e., RSV or taxi. In the simulation, $\hat{u}_i$ is set to follow a uniform distribution $U\left(\min\left\{\alpha^{\text{rsv}},\alpha^{\text{taxi}}\right\},u_{\max}\right)$ to distinguish the heterogeneity of passenger valuations across different travel purposes, where $u_{\max}$ denotes the highest valuation for unit trip distance. The range starts with $\min\left\{\alpha^{\text{rsv}},\alpha^{\text{taxi}}\right\}$ is aiming to ensure passengers who are willing to request hailing services would choose at least one hailing type in the beginning, i.e., ensuring $u_i(0) \geq \min\left\{\alpha^{\text{rsv}},\alpha^{\text{taxi}}\right\}$. Accordingly, the passenger's hailing type choice can be determined by the following Eq. (8).

$$\text{Hailing type at } t = \begin{cases} \text{only RSV}, & \text{if } \alpha^{\text{rsv}} \leq u_i(t) < \alpha^{\text{taxi}} \\ \text{only taxi}, & \text{if } \alpha^{\text{taxi}} \leq u_i(t) < \alpha^{\text{rsv}} \\ \text{both RSV and taxi}, & \text{if } \alpha^{\text{rsv}} \leq u_i(t) \text{ and } \alpha^{\text{taxi}} \leq u_i(t) \end{cases}. \tag{8}$$

For example, suppose passenger *k* has a 10-unit distance hailing request with $\hat{u}_k = 2$ and $\beta_{\text{sunk}}^{\text{pas}} = 0.2$. The fare rates $\alpha^{\text{rsv}} = 1$ and $\alpha^{\text{taxi}} = 3$. Initially, $u_k(0) = 2$, passenger *k* only requests RSV service since $\alpha^{\text{rsv}} < u_k(0) < \alpha^{\text{taxi}}$. After this, if the passenger has not been matched with any RSV until *t* = 5, then passenger *k* would request both RSV and taxi services because $\alpha^{\text{rsv}} < \alpha^{\text{taxi}} = u_k(5) = 3$.

Our proposed method is more general than existing studies (Wang et al., 2020; Yu et al., 2020; Xu et al., 2022) by adopting a linear function to characterize the effect of waiting time on passenger *i*'s hailing type decision via Eq. (7). That is to say, if one selected type of hailing vehicle is not available for a long time, the mental accounting utility of a passenger may be increased by the sunk time cost, leading him/her to request more hailing types. Ülkü et al. (2020) also suggest that people who spend a longer time waiting in line tend to consume more. In practice, a TNC, like DiDi, currently allows passengers to append the hailing types they prefer via its smartphone application.

Note that if a passenger requests both RSV and taxi services and there are available vehicles for both hailing types, then the TNC will match the passenger with the closest vehicle. If both types of closest vehicles are at the same distance from the passenger, then the less expensive one will be matched. Further, if the fares of both types of closest vehicles are the same, then the match is randomized.

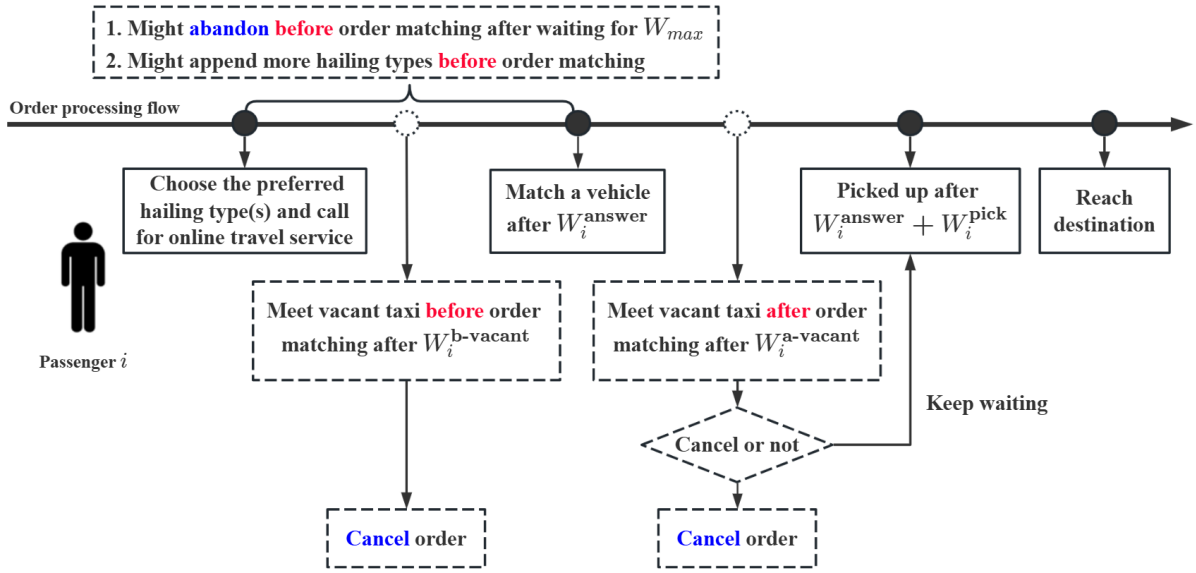

Fig. 5. Example of the hailing service process

The whole hailing service process is illustrated in Fig. 5. Initially, passenger *i* determines the preferred hailing type(s) with $u_i(0)$ via Eq. (8), and sends an online travel request to the TNC. Note that the passenger might append more hailing types before order matching. Ideally, the TNC matches the request with a vehicle, either an RSV or a hybrid taxi. Then, the matched vehicle arrives at passenger *i*'s origin, the passenger boards the vehicle, travels to the destination, and the service ends. During such a process, the time difference between passenger *i* submitting the request and receiving the matched vehicle is the answer time, W_i^{answer}; the elapsed time between passenger *i* matching to and boarding on the matched vehicle is the pick-up time, W_i^{pick}.

In the process, there are three main occasions when a passenger may cancel his/her request.

First, before an order is matched, a passenger abandons the request upon exhausting his/her patience. Specifically, if the answer time W_i^{answer} for the TNC to match passenger *i* with a vehicle

exceeds the passenger's maximum patience time $W_{\max}$ (i.e., $W_i^{\text{answer}} > W_{\max}$), the request is abandoned and he/she will take public transit to complete the trip. This reflects the natural decline in passenger patience as waiting time increases.

Second, before an order is matched, a passenger cancels the request once he/she encounters a cruising vacant taxi after waiting for $W_i^{\text{b-vacant}}$ minutes while he/she is also opting for taxi service. This decision is driven by two factors: first, taking the available taxi ensures an earlier arrival at the destination; second, passengers tend to have lower patience before their ride is confirmed (Xu et al., 2021a). Psychologically, uncertain waiting times feel longer than certain ones (Maister, 1984).

Third, after the order is matched, a passenger who is willing to accept taxi service may cancel the order when he/she encounters a cruising vacant taxi. The decision depends on the utility difference between completing the trip with the matched vehicle and opting for cruising taxis. The two utilities are mathematically expressed in the following two equations, respectively.

$$C_i^1 = \begin{cases} \beta_{\text{time}}^{\text{pas}} \left(W_i^{\text{answer}} + W_i^{\text{pick}} - W_i^{\text{a-vacant}} \right) + \alpha^{\text{rsv}} l_i, & \text{if matched with RSV} \\ \beta_{\text{time}}^{\text{pas}} \left(W_i^{\text{answer}} + W_i^{\text{pick}} - W_i^{\text{a-vacant}} \right) + \alpha^{\text{taxi}} l_i, & \text{if matched with hybrid taxi} \end{cases}, \tag{9}$$

$$C_i^2 = \alpha^{\text{taxi}} l_i + \hat{p} + H \cdot \tag{10}$$

In Eq. (9), the first part of the right side represents the remaining waiting time cost for the matched vehicle, where $\beta_{\text{time}}^{\text{pas}}$ is the passengers' time cost coefficient, $W_i^{\text{a-vacant}}$ denotes the waiting time when passenger *i* encounters a vacant taxi after order matching. The second part represents the fare cost.

In Eq. (10), the first part of the right side represents the fare cost of taking a vacant taxi, $\hat{p}$ is the penalty a passenger has to pay for canceling a matched order, and H is the corresponding psychological cost (He and Shen, 2015; He et al., 2018; Wang et al., 2020; Li et al., 2023a).

It is worth noting that if a passenger encounters a vacant taxi before the matched vehicle arrives and decides to continue waiting, he/she will consistently wait for the matched vehicle, even if other vacant taxis appear before then. This behavior can be explained as follows. Suppose passenger *i* is matched with an RSV and encounters a vacant taxi after order matching. If the passenger chooses to continue waiting at this moment, it implies that $C_i^1 \le C_i^2$. Let $C_i^{1+} = \beta_{\text{time}}^{\text{pas}}(W_i^{\text{answer}} + W_i^{\text{pick}}) + \alpha^{\text{rsv}} l_i$. Then, $C_i^1 = C_i^{1+} - \beta_{\text{time}}^{\text{pas}} \cdot W_i^{\text{a-vacant}}$. Let $W_{i2}^{\text{a-vacant}}$ denote the time at which passenger *i* encounters another vacant taxi after choosing to continue waiting for the first time, and let C_{i2}^1 represent the utility of passenger *i* choosing to continue waiting for the second time after order matching. Thus, we have $C_{i2}^1 = C_i^{1+} - \beta_{\text{time}}^{\text{pas}} \cdot W_{i2}^{\text{a-vacant}}$. Since $W_{i,2}^{\text{a-vacant}} > W_i^{\text{a-vacant}}$, it follows that $C_i^{1+} - \beta_{\text{time}}^{\text{pas}} \cdot W_{i,2}^{\text{a-vacant}} < C_i^{1+} - \beta_{\text{time}}^{\text{pas}} \cdot W_i^{\text{a-vacant}}$. Therefore, we can obtain $C_{i,2}^1 < C_i^1 \le C_i^2$, meaning that if passenger *i* chooses to continue waiting for the first time, he/she will keep waiting until the matched RSV arrives. The same reasoning applies to passengers matched with hybrid taxis.

4.2 Objective functions

This section formulates the four objective functions for passengers, taxi drivers, RSV drivers, and the TNC, respectively. Each objective is modeled and evaluated within a single time interval.

(1) Average hailing cost of passengers

From the passengers' perspective, the objective is to minimize the average hailing cost. Mathematically, this is expressed as:

$$\overline{C} = \frac{1}{N(T,\lambda)} \sum_{i=1}^{N(T,\lambda)} C_i , \tag{11}$$

where $N(T,\lambda)$ denotes the number of passengers who arrived and ended hailing service at the hailing demand rate λ during a time interval T. C_i is the generalized hailing cost associated with passenger i and is calculated based on the selected hailing services. Mathematically, it is given by,

$$C_i = \begin{cases} \beta_{\text{time}}^{\text{pas}} \left(W_i^{\text{answer}} + W_i^{\text{pick}} + l_i / v \right) + \alpha^{\text{taxi}} l_i, & i \in G^{\text{h-taxi}} \\ \beta_{\text{time}}^{\text{pas}} \left(W_i^{\text{answer}} + W_i^{\text{pick}} + l_i / v \right) + \alpha^{\text{rsv}} l_i, & i \in G^{\text{rsv}} \\ \beta_{\text{time}}^{\text{pas}} \left(W_i^{\text{b-vacant}} + l_i / v \right) + \alpha^{\text{taxi}} l_i, & i \in G_{\text{cancel}} \\ \beta_{\text{time}}^{\text{pas}} \left(W_i^{\text{a-vacant}} + l_i / v \right) + \alpha^{\text{taxi}} l_i + H + \hat{p}, & i \in G_{\text{cancel}}^{\text{h-taxi}} \cup G_{\text{cancel}}^{\text{rsv}} \\ \beta_{\text{time}}^{\text{pas}} \left(W_{\max} + \overline{W}^{\text{tansit}} + l_i / v^{\text{tansit}} \right) + \alpha^{\text{tansit}} l_i + \beta_{\text{time}}^{\text{pas}} \left(l_i / v^{\text{tansit}} - l_i / v \right), & i \in G_{\text{abandon}} \end{cases} , \tag{12}$$

where $G^{\text{h-taxi}}$ and G^{rsv} denote the sets of passengers served by hybrid taxi and RSV through online matching, respectively; G_{cancel} denotes the set of passengers who canceled their requests before order matching; $G_{\text{cancel}}^{\text{h-taxi}}$ and $G_{\text{cancel}}^{\text{rsv}}$ denote the sets of passengers who canceled hybrid taxi and RSV orders after order matching, respectively; G_{abandon} denotes the set of passengers who abandoned their online requests. For abandoned passengers, let $\beta_{\text{time}}^{\text{pas}} \left(l_i / v^{\text{tansit}} - l_i / v \right)$ denote an additional penalty item to represent the loss of failing to get hailing services, which means the extra time cost of taking public transit compared to hailing services.

For the split of travel demand, the hailing demand rate λ is calculated as below,

$$\lambda = \Lambda \frac{\exp\left(-\theta^{\text{pas}} \overline{L}\right)}{\exp\left(-\theta^{\text{pas}} \overline{L}\right) + \exp\left(-\theta^{\text{pas}} \overline{C}^{\text{transit}}\right)}, \tag{13}$$

$$\overline{C}^{\text{transit}} = \beta_{\text{time}}^{\text{pas}} \left(\overline{W}^{\text{tansit}} + \overline{l} / v^{\text{tansit}} \right) + \alpha^{\text{transit}} \overline{l} \tag{14}$$

$$\overline{L} = \frac{1}{\theta_0} \ln \left\{ \exp\left(\theta_0 \overline{C}^{\text{rsv}}\right) + \exp\left(\theta_0 \overline{C}^{\text{taxi}}\right) \right\}, \tag{15}$$

where θ^{pas} is the dispersion coefficient in the Logit model; $\overline{C}^{\text{transit}}$ is the average travel cost associated

with public transit services; $\overline{L}$ represents the logsum of the disutility as perceived by the passenger who decides to take hailing services to fulfill the travel demand (Ben-Akiva and Lerman, 1985; He et al., 2018), where θ_0 is the logsum parameter, $\overline{C}^{\text{rsv}}$ and $\overline{C}^{\text{taxi}}$ represent the average travel costs of passengers who are served by RSVs and taxis, respectively, which can be calculated by the following equations.

$$\overline{C}^{\text{rsv}} = \frac{\sum_{i \in G^{\text{rsv}}} C_i}{\left| G^{\text{rsv}} \right|}, \tag{16}$$

$$\overline{C}^{\text{taxi}} = \frac{\sum_{i \in G^{\text{h-taxi}} \cup G_{\text{cancel}} \cup G_{\text{cancel}}^{\text{h-taxi}} \cup G_{\text{cancel}}^{\text{rsv}}} C_i}{\left| G^{\text{h-taxi}} \cup G_{\text{cancel}} \cup G_{\text{cancel}}^{\text{h-taxi}} \cup G_{\text{cancel}}^{\text{rsv}} \right|}. \tag{17}$$

(2) Average profit of taxi drivers

For taxi drivers, their objective is to maximize the average profit, computed by,

$$Q^{\text{taxi}} = \frac{\tau^{\text{taxi}} \left(\sum_{i \in G^{\text{h-taxi}}} \alpha^{\text{taxi}} l_i + \sum_{i \in G_{\text{cancel}}^{\text{h-taxi}}} \hat{p} \right) - \sum_{i \in G_{\text{cancel}}^{\text{h-taxi}}} \beta^{\text{h-taxi}} \left(W_i^{\text{a-vacant}} - W_i^{\text{answer}} \right) + \sum_{i \in G_{\text{street}}^{\text{h-taxi}}} \alpha^{\text{taxi}} l_i + \sum_{i \in G^{\text{s-taxi}}} \alpha^{\text{taxi}} l_i}{Z^{\text{taxi}}} - \left(vT\gamma + \hat{\gamma}^{\text{taxi}} \right), \tag{18}$$

where Z^{taxi} is the number of total taxis; τ^{taxi} is the wage rate paid by the TNC to hybrid taxi drivers; $G_{\text{street}}^{\text{h-taxi}}$ denotes the set of passengers served by hybrid taxis on the street; $G^{\text{s-taxi}}$ denotes the set of passengers served by street taxis; γ is the fuel cost per unit distance of hailing vehicles; $\hat{\gamma}^{\text{taxi}}$ is the fixed operating cost of taxis (representing the cost of taxicab license fee, insurance, depreciation evenly distributed over single time interval); $\beta^{\text{h-taxi}}$ is the time cost coefficient of hybrid taxi drivers, which represents the potential income per unit of time wasted by passengers' cancellation. Let $Z^{\text{h-taxi}}$ and $Z^{\text{s-taxi}}$ be the number of hybrid and street taxis in the system, respectively, $Z^{\text{h-taxi}} + Z^{\text{s-taxi}} = Z^{\text{taxi}}$. Then, $\beta^{\text{h-taxi}}$ can be formulated as follows,

$$\beta^{\text{h-taxi}} = \frac{\tau^{\text{taxi}} \left(\sum_{i \in G^{\text{h-taxi}}} \alpha^{\text{taxi}} l_i + \left| G_{\text{cancel}}^{\text{h-taxi}} \right| \cdot \hat{p} \right) + \sum_{i \in G_{\text{street}}^{\text{h-taxi}}} \alpha^{\text{taxi}} l_i}{Z^{\text{h-taxi}} \cdot T}. \tag{19}$$

Taxi drivers are assumed to update their work modes at the beginning of each time interval and maintain them throughout the interval. We then employ a Logit model to approximate the work mode split of taxi drivers (He and Shen, 2015; Wang et al., 2016):

$$Z^{\text{h-taxi}} = Z^{\text{taxi}} \frac{\exp\left(\theta^{\text{taxi}} Q^{\text{h-taxi}} \right)}{\exp\left(\theta^{\text{taxi}} Q^{\text{h-taxi}} \right) + \exp\left(\theta^{\text{taxi}} Q^{\text{s-taxi}} \right)}, \tag{20}$$

$$Z^{\text{s-taxi}} = Z^{\text{taxi}} \frac{\exp\left(\theta^{\text{taxi}} Q^{\text{s-taxi}}\right)}{\exp\left(\theta^{\text{taxi}} Q^{\text{h-taxi}}\right) + \exp\left(\theta^{\text{taxi}} Q^{\text{s-taxi}}\right)}, \tag{21}$$

where θ^{taxi} is the dispersion coefficient, $Q^{\text{h-taxi}}$ and $Q^{\text{s-taxi}}$ are the average profits of hybrid and street taxi drivers in a modeling time interval, respectively. They can be calculated by the following equations.

$$Q^{\text{h-taxi}} = \frac{\tau^{\text{taxi}}\left(\sum_{i \in G^{\text{h-taxi}}} \alpha^{\text{taxi}} l_i + \left|G_{\text{cancel}}^{\text{h-taxi}}\right| \cdot \hat{p}\right) - \sum_{i \in G_{\text{cancel}}^{\text{h-taxi}}} \beta^{\text{taxi}}\left(W_i^{\text{a-vacant}} - W_i^{\text{answer}}\right) + \sum_{i \in G_{\text{street}}^{\text{h-taxi}}} \alpha^{\text{taxi}} l_i}{Z^{\text{h-taxi}}} - \left(vT\gamma + \hat{\gamma}^{\text{taxi}}\right), \tag{22}$$

$$Q^{\text{s-taxi}} = \frac{\sum_{i \in G^{\text{s-taxi}}} \alpha^{\text{taxi}} l_i}{Z^{\text{s-taxi}}} - \left(vT\gamma + \hat{\gamma}^{\text{taxi}}\right). \tag{23}$$

(3) Average profit of RSV drivers

The objective of RSV drivers is also to maximize the average profit within a modeling time interval. Mathematically, it is expressed by,

$$Q^{\text{rsv}} = \frac{\tau^{\text{rsv}}\left(\sum_{i \in G^{\text{rsv}}} \alpha^{\text{rsv}} l_i + \left|G_{\text{cancel}}^{\text{rsv}}\right| \cdot \hat{p}\right) - \sum_{i \in G_{\text{cancel}}^{\text{rsv}}} \beta^{\text{rsv}}\left(W_i^{\text{a-vacant}} - W_i^{\text{answer}}\right)}{Z^{\text{rsv}}} - \left(vT\gamma + \hat{\gamma}^{\text{rsv}}\right), \tag{24}$$

where $\hat{\gamma}^{\text{rsv}}$ is the fixed operating cost of RSVs (representing the cost of insurance and depreciation evenly distributed over one time interval); β^{rsv} is the time cost coefficient of the RSV drivers, which is given by

$$\beta^{\text{rsv}} = \frac{\tau^{\text{rsv}}\left(\sum_{i \in G^{\text{rsv}}} \alpha^{\text{rsv}} l_i + \left|G_{\text{cancel}}^{\text{rsv}}\right| \cdot \hat{p}\right)}{Z^{\text{rsv}} \cdot T}. \tag{25}$$

(4) Profit of the TNC

The TNC generates income by charging passengers trip fares and collecting penalties when passengers cancel matched orders. Its cost arises from paying wages to RSV and hybrid taxi drivers. The objective of the TNC is to maximize its profit, which is:

$$Q^{\text{TNC}} = \left(1 - \tau^{\text{taxi}}\right)\left(\sum_{i \in G^{\text{h-taxi}}} \alpha^{\text{taxi}} l_i + \left|G_{\text{cancel}}^{\text{h-taxi}}\right| \cdot \hat{p}\right) + \left(1 - \tau^{\text{rsv}}\right)\left(\sum_{i \in G^{\text{rsv}}} \alpha^{\text{rsv}} l_i + \left|G_{\text{cancel}}^{\text{rsv}}\right| \cdot \hat{p}\right). \tag{26}$$

4.3 Solution Method

Solving the proposed bi-level model (Eq. (1)–(4)) is challenging. First, the proposed problem includes multiple objectives and decision variables, leading to a high computational complexity. Second, the lower-level problem involves complex interactions and behaviors of passengers and drivers, which are difficult to analytically formulate, making it challenging to derive closed-form solutions or apply tractable solution methods. Hence, we develop a solution approach based on the multi-objective Bayesian optimization to solve this problem (Fig. 6). The merit of using Bayesian optimization to address black-box bi-level optimization is avoiding frequent calls to the lower-level simulation via constructing a surrogate model. The surrogate model approximates the lower-level model with an analytical function based on a small amount of sample data. Then, new candidate solutions, which are promising to achieve an improvement in the Pareto frontier, are generated based on the acquisition function.

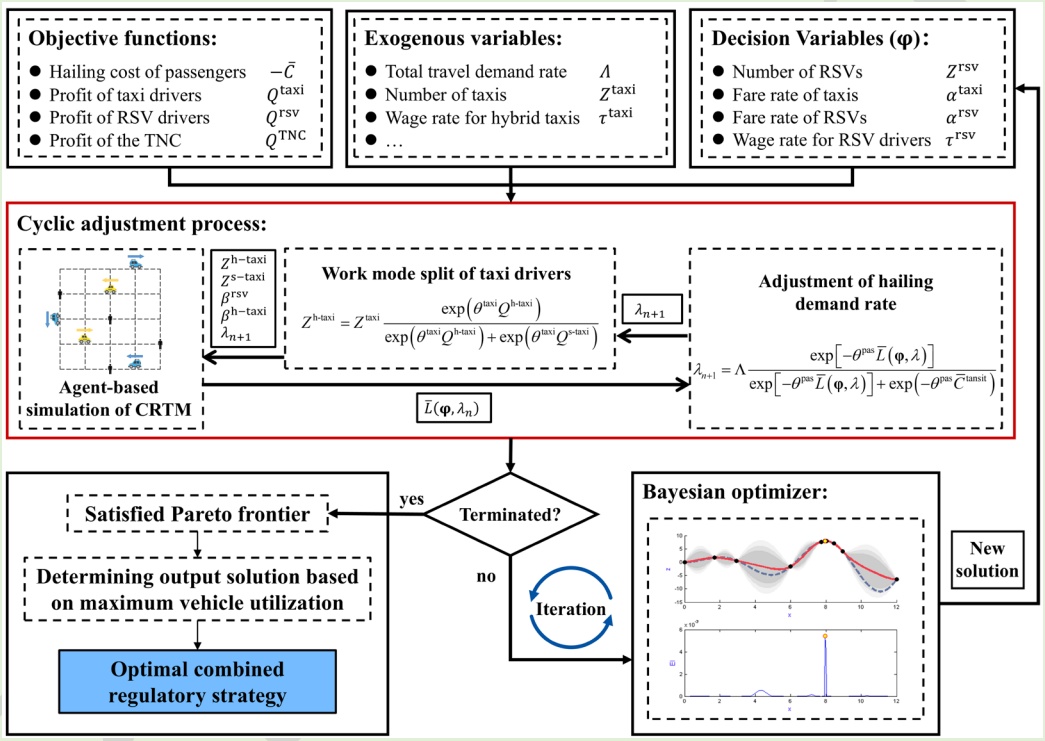

Fig. 6. A multi-objective Bayesian optimization based solution framework for optimizing the combined regulatory strategy of CRTM

As discussed in Section 1, when optimizing the combined regulatory strategy, it is necessary to evaluate the market performance with stable supply-demand patterns and obtain a stabilized hailing demand rate $\lambda^*(\boldsymbol{\varphi})$ and work mode split of taxi drivers under a given regulatory strategy $\boldsymbol{\varphi}$. Let $\bar{L}(\boldsymbol{\varphi}, \lambda)$ denote the logsum disutility of hailing passengers under strategy $\boldsymbol{\varphi}$ and demand rate λ. Here $\bar{L}(\boldsymbol{\varphi}, \lambda)$ is a function of λ. Note that in Eq. (13), λ is also a function of $\bar{L}$. This results in a fixed-point problem. Following existing studies that addressed similar fixed-point problems in transportation simulation research (Flötteröd, 2017; Wen et al., 2018), we iteratively run the model to adjust hailing demand rate until convergence, and then, output the corresponding objective values for further analysis or optimization. The iterative adjustment process for determining the endogenously stable hailing

demand rate $\lambda^*(\boldsymbol{\varphi})$ can be described as follows.

Define a sequence of real numbers $\{\lambda_n\}$, where $\lambda_n \geq 0$ denotes the n^{th} adjusted hailing demand rate at each iteration of the overall optimization process, we have:

$$\lambda_{n+1} = \Lambda \frac{\exp\left[-\theta^{\text{pas}} \bar{L}(\boldsymbol{\varphi}, \lambda)\right]}{\exp\left[-\theta^{\text{pas}} \bar{L}(\boldsymbol{\varphi}, \lambda)\right] + \exp\left(-\theta^{\text{pas}} \bar{C}^{\text{tansit}}\right)}, \tag{27}$$

where the constants $\Lambda > 0$, $\theta^{\text{pas}} > 0$, $\bar{C}^{\text{tansit}} > 0$.

As shown in the red box in Fig. 6, after each adjustment of the hailing demand rate, the first step is to determine the work mode split of taxi drivers, which is influenced by decision variables and the hailing demand rate. Then, the logsum disutility of hailing passengers calculated from the agent-based simulation is fed back into Eq. (27) for the next adjustment. This iterative process terminates when the adjusted hailing demand rate reaches the convergence condition. Then, the four corresponding objective values are calculated and substituted into the Bayesian optimizer to acquire the next candidate solution. Note that the hailing demand rate implies the average arriving number of passengers who request hailing services per time stamp. In this study, we set the convergence condition to be $|\lambda_n - \lambda_{n-1}| < 1$ (request/min), $n \geq 1$, which means the iterative adjustment process stops when the absolute difference between consecutive adjusted λ values does not exceed one passenger during each iteration.

After several iterations of the overall multi-objective Bayesian optimization, we can obtain a stabilized Pareto frontier with multiple non-dominated solution points. Then, the final Pareto optimal output solution $\boldsymbol{\varphi}^*$ is determined by a secondary criterion of maximizing total vehicle utilization.

4.4 Multi-objective Bayesian optimization

4.4.1 Surrogate model

The first step in the multi-objective Bayesian optimization is constructing a surrogate model based on the sampled data. This paper employs the Gaussian process regression as the surrogate model to fit the complex nonlinear relationship between the decision variables and the multi-objective functions (Rasmussen, 2003; Frazier, 2018).

Consider a set of decision variables $\mathbf{X}_m = (\mathbf{x}_1, \ldots, \mathbf{x}_m)^\top = \begin{pmatrix} x_{1,1} & \cdots & x_{1,d} \\ \vdots & \ddots & \vdots \\ x_{m,1} & \cdots & x_{m,d} \end{pmatrix}$ with m samples in d dimensions ($d = 4$ in this paper) and an associated set of objective function values $\mathbf{f}_m^\omega = \left(f^\omega(\mathbf{x}_1), \ldots, f^\omega(\mathbf{x}_m)\right)^\top$, $\omega = 1, 2, 3, 4$. Note that x corresponds to a regulatory strategy and f corresponds to an objective function in this study. For example, $x_{2,1}$ means the number of RSVs Z^{rsv} in the 2nd sample point, $f^2(\mathbf{x}_1)$ indicates the average profit of taxi drivers under the 1st sample decision

variable vector $\mathbf{x}_1 = \left(x_{1,1}, x_{1,2}, x_{1,3}, x_{1,4}\right)$.

Taking the ω^{th} objective as an example, the Gaussian process assumes that for any given m, $\mathbf{f}_m^{\omega}$ follows an m-dimensional multivariate Gaussian distribution (Zhong et al., 2021; Huo et al., 2023a; Huo et al., 2023b):

$$\mathbf{f}_m^{\omega} \sim \mathcal{N}\left(\boldsymbol{\mu}_m^{\omega}, \mathbf{K}_m\right), \tag{28}$$

where $\boldsymbol{\mu}_m^{\omega} = \left(E\left(f^{\omega}\left(\mathbf{x}_1\right)\right), \ldots, E\left(f^{\omega}\left(\mathbf{x}_m\right)\right)\right)^{\top}$, $E(\cdot)$ denotes the expected value of the objective function. $\mathbf{K}_m = \left(\mathbf{k}_1, \ldots, \mathbf{k}_m\right)^{\top} = \begin{pmatrix} k\left(\mathbf{x}_1, \mathbf{x}_1\right) & \cdots & k\left(\mathbf{x}_1, \mathbf{x}_m\right) \\ \vdots & \ddots & \vdots \\ k\left(\mathbf{x}_m, \mathbf{x}_1\right) & \cdots & k\left(\mathbf{x}_m, \mathbf{x}_m\right) \end{pmatrix}$, where $k(\cdot,\cdot)$ is the covariance kernel function. In this study, the common Matérn 5/2 kernel is used as the covariance kernel function:

$$k\left(\mathbf{x}, \mathbf{x}'\right) = \left(1 + \frac{\sqrt{5}\kappa}{\zeta} + \frac{5\kappa^2}{3\zeta^2}\right) \exp\left(-\frac{\sqrt{5}\kappa}{\zeta}\right), \tag{29}$$

where $\kappa = \left|\mathbf{x} - \mathbf{x}'\right|$, ζ is the hyperparameter that determines the Gaussian process curve, determined by maximizing the log-marginal likelihood function as follows:

$$\log p\left(\mathbf{f}_m^{\omega} \middle| \mathbf{X}_m\right) = -\frac{1}{2}\left(\mathbf{f}_m^{\omega}\right)^{\top} \mathbf{K}_m^{-1} \mathbf{f}_m^{\omega} - \frac{1}{2}\log\left|\mathbf{K}_m\right| - \frac{m}{2}\log 2\pi . \tag{30}$$

Given a sampling point $\mathbf{x}_{m+1}$, the objective values predicted by the Gaussian process satisfy the following distribution:

$$f^{\omega}\left(\mathbf{x}_{m+1}\right) \sim \mathcal{N}\left(\mu_{m+1}^{\omega}, \sigma_{m+1}^{\omega}\right), \tag{31}$$

where $\mu_{m+1}^{\omega} = \mathbf{k}_{m+1}^{\top} \mathbf{K}_m^{-1} \mathbf{f}_m^{\omega}$ and $\sigma_{m+1}^{\omega} = k\left(\mathbf{x}_{m+1}, \mathbf{x}_{m+1}\right) - \mathbf{k}_{m+1}^{\top} \mathbf{K}_m^{-1} \mathbf{k}_{m+1}$.

4.4.2 Acquisition function

The second step of multi-objective Bayesian optimization is to acquire the next candidate solution in the solution space based on the acquisition function that maximizes the improvement of the Pareto frontier, which can also reduce calls to the lower-level model. This paper adopts hypervolume-based probability of improvement (HVPoI) as the acquisition function to handle this multi-objective problem. Hypervolume (HV) is widely used in multi-objective optimization (Beume et al., 2007), and HVPoI can significantly reduce the overall computational complexity while retaining the advantages of using HV (Couckuyt et al., 2014). The specific computational steps are as follows.

Step 1. Calculate the probability of improvement.

Given $\mathbf{X}_m$, the initial Pareto frontier $\mathbb{P}$ can be expressed as:

$$\mathbb{P}=\left\{\mathbf{f}\left(\mathbf{x}_1^*\right),\ldots,\mathbf{f}\left(\mathbf{x}_q^*\right)\right\}, \tag{32}$$

where $q \le m$ is the number of Pareto optimal (non-dominated) solutions, for $i=1,\ldots,q$, $\mathbf{f}\left(\mathbf{x}_i^*\right)=\left(f^1\left(\mathbf{x}_i^*\right),\ldots,f^4\left(\mathbf{x}_i^*\right)\right)$, $\mathbf{x}_i^* \in \mathbf{X}_m$. The probability that a new sampled solution is in the non-dominated objective function space A is:

$$P(\mathbf{x})=\int_{\mathbf{f}(\mathbf{x})\in A}\prod_{\omega=1}^{4}\phi^{\omega}\left[f^{\omega}(\mathbf{x})\right]df^{\omega}(\mathbf{x}), \tag{33}$$

where $\phi^{\omega}(\mathbf{x})$ denotes the probability density function of $f^{\omega}(\mathbf{x})$, which can also be viewed as the probability that the new sampled solution improves the Pareto frontier $\mathbb{P}$. In this paper, we use the method of Couckuyt et al. (2014) to decompose the integration region A into b (hyper-)rectangular cells, then $P(\mathbf{x})$ can be computed as follows:

$$P(\mathbf{x})=\sum_{a=1}^{b}\pm\prod_{\omega=1}^{4}\left(\Phi^{\omega}\left(U_a^{\omega}\right)-\Phi^{\omega}\left(L_a^{\omega}\right)\right), \tag{34}$$

where $\Phi^{\omega}(\cdot)$ denotes the cumulative distribution function of $f^{\omega}(\mathbf{x})$, U_a^{ω} and L_a^{ω} denote the upper and lower bounds of the ω^{th} objective in the rectangular cell a, respectively. Since the method of Couckuyt et al. (2014) may have overlapping cells, the algorithm can use the $\pm$ symbol to negate the overlapping contribution of some specific cells.

Step 2. Calculate the HV improvement caused by the objective value $\mathbf{f}(\mathbf{x})$ of the sampled solution to the Pareto frontier $\mathbb{P}$.

HV denotes the volume of the region dominated by the Pareto frontier $\mathbb{P}$, which is bounded by the reference point $\mathbf{f}_{\max}$ that is dominated by all the points of $\mathbb{P}$. Larger values of HV indicate a better Pareto frontier. The HV improvement of $\mathbf{f}(\mathbf{x})$ on the Pareto frontier $\mathbb{P}$ is defined as:

$$\mathbb{H}^{\text{imp}}\left(\mathbf{f}(\mathbf{x}),\mathbb{P}\right)=\mathbb{H}\left(\mathbb{P}\cup\left\{\mathbf{f}(\mathbf{x})\right\}\right)-\mathbb{H}(\mathbb{P}), \tag{35}$$

where $\mathbb{H}(\cdot)$ denotes the HV indicator. $\mathbb{H}^{\text{imp}}(\cdot)$ can be defined in terms of a non-negative scalar improvement function:

$$\mathbb{I}\left(\mathbf{f}(\mathbf{x}),\mathbb{P}\right)=\begin{cases}\mathbb{H}^{\text{imp}}\left(\mathbf{f}(\mathbf{x}),\mathbb{P}\right), & \text{if } \mathbf{f}(\mathbf{x}) \text{ is not dominated by } \mathbb{P}\\ 0, & \text{otherwise}\end{cases}. \tag{36}$$

Step 3. Create the HVPoI-based acquisition function.

To reduce the computational complexity, the HVPoI-based acquisition function can be expressed as:

$$P_{\mathrm{HV}}(\mathbf{x}) = \mathbb{I}\left(\boldsymbol{\mu}(\mathbf{x}), \mathbb{P}\right) \cdot P(\mathbf{x}), \tag{37}$$

where $\boldsymbol{\mu}(\mathbf{x}) = \left(\mu^1(\mathbf{x}), \ldots, \mu^4(\mathbf{x})\right)$. $P_{\mathrm{HV}}(\mathbf{x})$ can be calculated as follows:

$$P_{\mathrm{HV}}(\mathbf{x}) = \left(\sum_{a=1}^{b} \pm \mathbb{V}\left(\boldsymbol{\mu}(\mathbf{x}), \mathbf{U}_a, \mathbf{L}_a\right)\right) \cdot P(\mathbf{x}), \tag{38}$$

where $\mathbb{V}\left(\boldsymbol{\mu}(\mathbf{x}), \mathbf{U}_a, \mathbf{L}_a\right) = \begin{cases} \prod_{\omega=1}^{4}\left(U_a^{\omega} - \max\left(L_a^{\omega}, \mu^{\omega}(\mathbf{x})\right)\right), & \text{if } U_a^{\omega} > \mu^{\omega}(\mathbf{x}) \text{ for } \omega = 1,2,3,4 \\ 0, & \text{otherwise} \end{cases}$, $\mathbf{U}_a$ and $\mathbf{L}_a$ denote the sets of upper and lower bounds of the rectangular cell a, respectively.

5 Numerical experiments

In this section, we first validate the performance of the agent-based simulation model using real-world data. Then, the impact of each decision variable on different objective functions is investigated. After that, we present a case study to obtain the Pareto optimal combined regulatory strategy based on the proposed solution framework. Finally, we discuss the difference of optimizing regulatory strategies in a single-objective manner and examine the effects of ignoring passenger impatience.

The computations in this section were performed on a laptop equipped with an Intel Core Ultra 7 1.40 GHz CPU and 32 GB of RAM, and the simulation was coded based on Python. The details of the three main loops used in the following experiments are described in Appendix B.

5.1 Model validation

To validate the agent-based simulation model, we use the open dataset provided by DiDi, one of the largest TNCs in China. The dataset contains the number of requested orders, completed orders, and operating vehicles in a specific area of Hangzhou City every half-hour for two weeks in November 2018 (Fig. 7(a)). However, since this dataset lacks trip information for each order, we select the number of orders completed between 7:00 to 23:00 to be the indicator for validating the performance of our simulation, as this period is considered to be the main operating hours of hailing services. The length T of each time interval is set to be 30 (min), each minute indicates one time stamp in the simulation. Meanwhile, the passengers in the model are considered to be homogeneous in the maximum waiting time $W_{\max}$, the time cost coefficient $\beta_{\mathrm{time}}^{\mathrm{pas}}$, the sunk time cost coefficient $\beta_{\mathrm{sunk}}^{\mathrm{pas}}$, and the psychological cost H.

The pricing and wage parameters in the model are set based on the market pricing in Hangzhou. In 2018, the flag-down fee for Hangzhou taxis was 11 (¥/3km), which was about 3.6 (¥/km), and the taxi kilometer fee was 2.5 (¥/km)[1]. For the ridesourcing services, the flag-down fee for DiDi Express

[1] https://www.hangzhou.gov.cn/art/2019/10/30/art_1229063385_1721172.html

was 8 (¥/2.5km), which was about 3.2 (¥/km), and the ridesourcing kilometer fee was about 1.7 (¥/km)[2]. The average commission rate charged by DiDi to drivers was 19%, and an average of 7% of incentives were returned to drivers[3] in the 4th quarter of 2018. In the model, we approximate the fare rate of taxis $\alpha^{\text{taxi}} = 3.0$ (¥/km) and the fare rate of RSVs $\alpha^{\text{rsv}} = 2.5$ (¥/km), and we round up to a 90% wage rate τ^{rsv} for RSV drivers.

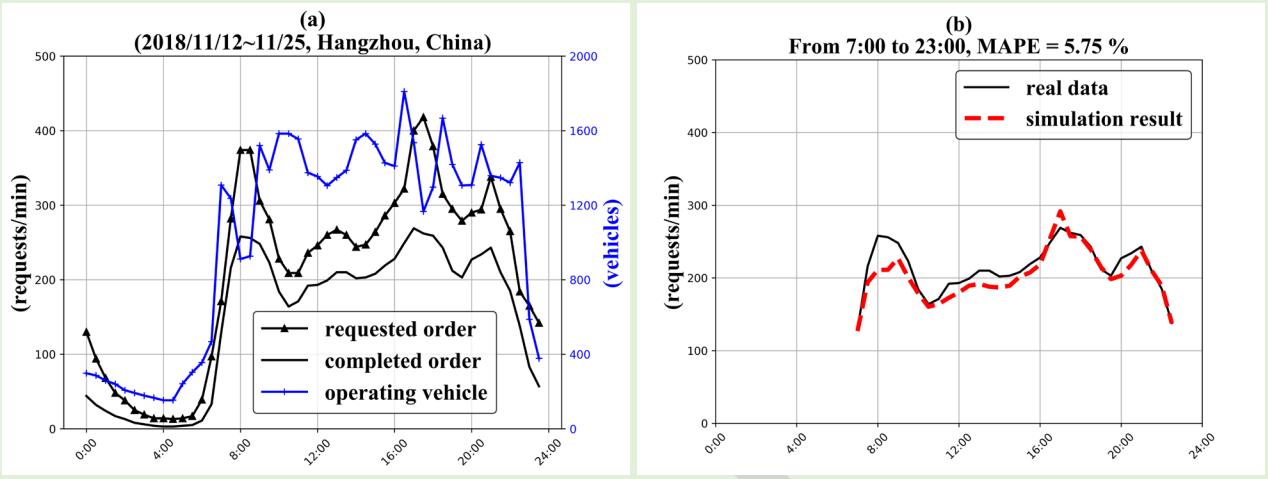

Fig. 7. (a) Average number of requested orders, completed orders, and operating vehicles at different day periods. (b) Comparison between the simulation results and the real data.

Due to privacy protection, geographic information is not provided in the DiDi dataset, so we estimate the scale of the road network M based on the number of RSVs. The maximum number of operating RSVs in the DiDi dataset between 7:00 to 23:00 is 1800, and the average number is 1400. In November 2018, there were about 25500 registered RSVs in Hangzhou[4]. Meanwhile, the central urban area of Hangzhou City is 1031 (km^2)[5]. Then, based on the maximum number of RSVs in the dataset, the area of the study region is estimated to be 72.7 (km^2), which is proportionally computed via $1800\times1031/25500 \approx 72.7$. Accordingly, we obtained the side length of the study region as 8.5 (km) by taking the square root of 72.7. Let the length of each grid in the simulation be 0.5 (km), then a 17×17 grid-type road network is employed to simulate the study region, i.e., $M = 17$. Furthermore, there were 11300 taxis in the central urban area of Hangzhou in 2018[6]. We proportionally compute the number of taxis in the study region via $1800\times11300/25500 \approx 814$. Other parameter settings and corresponding sources/references are provided in Appendix C. Moreover, we define a benchmark case $\boldsymbol{\varphi}_0$ based on the above market scenario, in which $Z^{\text{rsv}} = 1400$ (veh), $\alpha^{\text{taxi}} = 3.0$ (¥/km), $\alpha^{\text{rsv}} = 2.5$ (¥/km), and $\tau^{\text{rsv}} = 90\%$.

Based on the proceeding settings, we run the simulation using Algorithm B.2 and obtain the number of completed orders between 7:00 to 23:00. For each run, the average number of requested

[2] https://www.263th.com/shouqi/126708.html
[3] https://www.sohu.com/a/309891044_250147
[4] https://hznews.hangzhou.com.cn/chengshi/content/2018-08/30/content_7059606.htm
[5] http://ghzy.hangzhou.gov.cn/art/2020/1/9/art_1228962782_41563990.html
[6] http://hangzhouds.org.cn/HangzhouBook/info.aspx?itemid=1197&page=1

orders and operating vehicles in the DiDi dataset are respectively converted to the hailing demand rate $\hat{\lambda}$ and the number of RSVs $\hat{Z}^{rsv}$ as the input for Algorithm B.2. Refer to Wei et al. (2022), the Mean Absolute Percentage Error (MAPE) is adopted to evaluate the performance of the simulation. As illustrated in Fig. 7(b), the MAPE between the simulation result and real data is 5.75%, which shows a satisfactory performance. However, there is a significant difference during the morning peak period. A possible reason is that in 2018, most RSV drivers were part-time and had their own family commuting needs (Qi and Li, 2020), causing the number of operating RSVs from the DiDi dataset to be smaller in the morning peak than in the afternoon.

Furthermore, we also examine an important indicator that has received much attention in the literature, i.e., the average waiting time of passengers. Let the hailing demand rate λ varies between 0 and 500 (requests/min), we run Algorithm B.2 under the benchmark market case $\boldsymbol{\varphi}_0$. Fig. 8(a) shows the average waiting times of all passengers and passengers served by RSVs, hybrid taxis online, and cruising taxis under different hailing demand rates. Note that passengers served by cruising taxis include both those served by street taxis and those served by hybrid taxis while cruising. As the hailing demand rate λ increases, all kinds of average waiting times show an overall increasing trend.

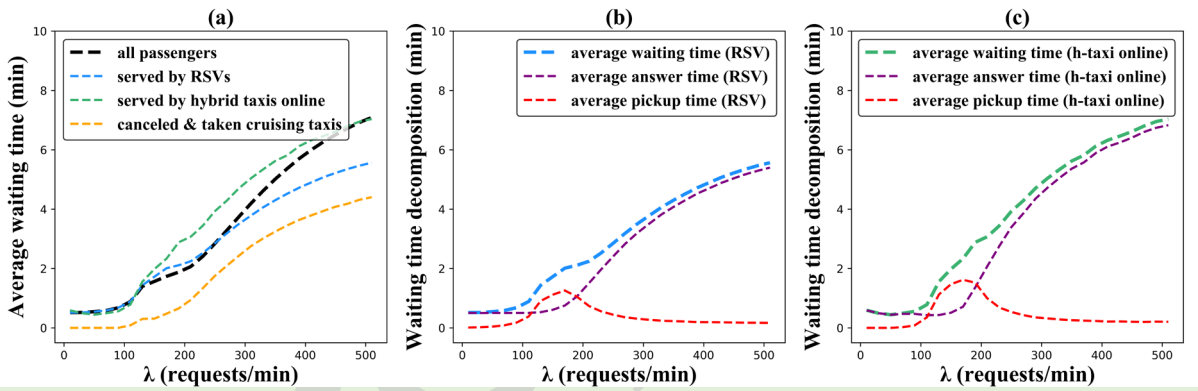

Fig. 8. (a) Average waiting times of passengers served by different carriers. (b) Waiting time decomposition of RSV passengers. (c) Waiting time decomposition of hybrid taxi passengers.

Notably, after decomposing the average waiting times of RSV and online taxi passengers into the answer time and the pick-up time (Fig. 7(b) and (c)), it is found that the average pick-up time shows a significant non-monotonicity. Since the speed of vehicles is set to be fixed, that implies the average distance between passengers and their matched vehicles is similarly non-monotonic. An explanation for this phenomenon is that as λ increases at first, the number of available vehicles in the system decreases, and the average distance between passengers and their matched vehicles gradually increases. When λ reaches a certain level, it becomes difficult to match newly arriving passengers to available vehicles directly, and the average answer time of passengers begins to increase. Further, as the passenger density in the network keeps increasing, the distance to the nearest passenger decreases when a vehicle becomes available, which leads to a non-monotonic pick-up time. The significant non-monotonicity in the average pick-up time is also reached by Castillo et al. (2017) and Feng et al. (2021), which further supports the validity of the model presented in this study.

5.2 Impact of regulatory strategies

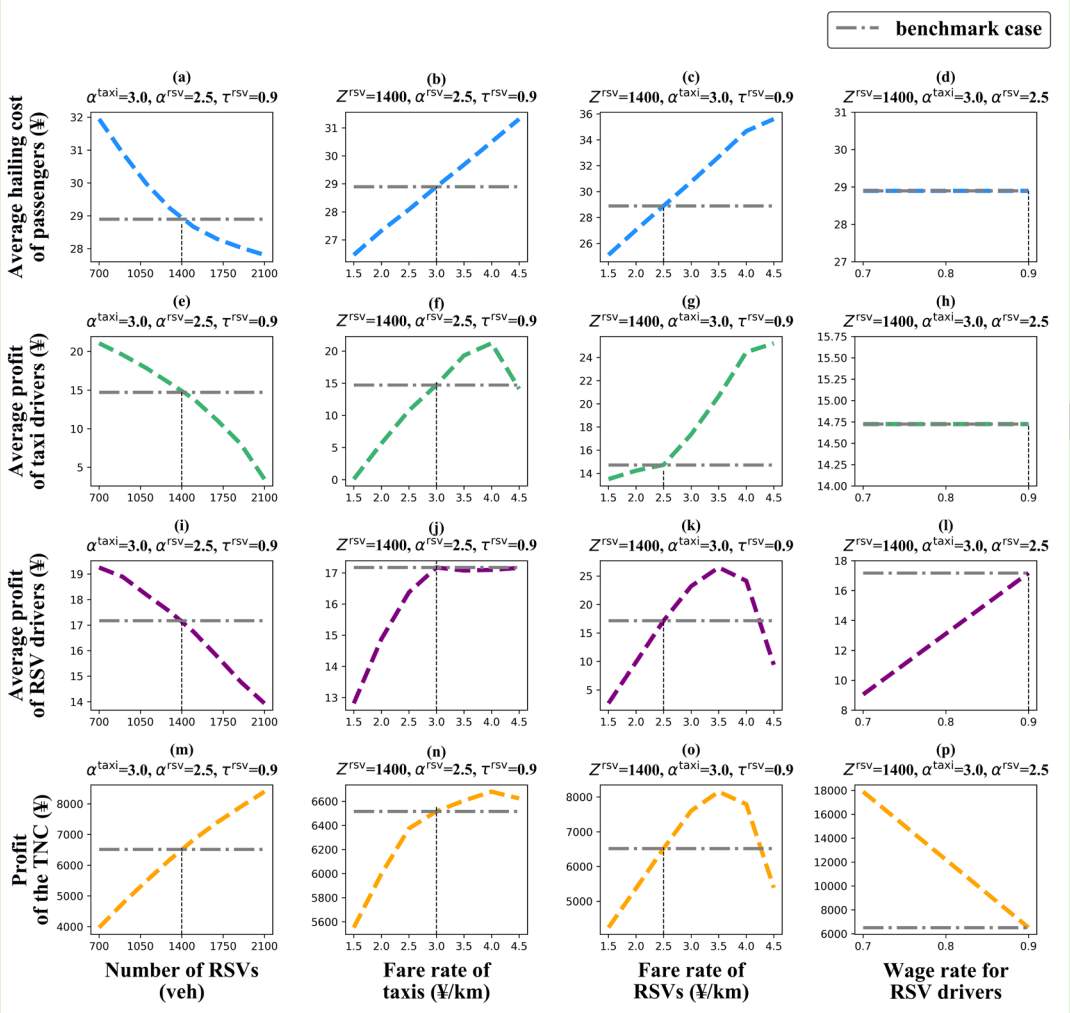

Fig. 9. Relationships between decision variables and objective functions.

Fig. 9 illustrates the impact of the number of RSVs Z^{rsv}, the fare rate of taxis α^{taxi}, the fare rate of RSVs α^{rsv}, and the wage rate for RSV drivers τ^{rsv} on the objective functions of different stakeholders. Each subfigure is examined by varying a single decision variable while keeping the others remain benchmark setting, and the results are computed using Algorithm B.3. From Fig. 9, it is evident that an increase or decrease in any of the decision variables does not benefit passengers, taxi drivers, RSV drivers, and the TNC simultaneously. Taking the regulation of the RSV number as an example, when the number of RSVs decreases, the average profits of both taxi and RSV drivers increase (Fig. 9(e) and (i)), but both passengers and the TNC experience negative effects (Fig. 9(a) and (m)). Conversely, an increase in the number of RSVs benefits both passengers and the TNC, but it results in a decrease in the average profits of both taxi and RSV drivers (Fig. 9(e) and (i)), which reflects the fact that unregulated growth in the number of RSVs leads to a loss of profit for both taxis and RSV drivers.

Notably, the average profit of taxi drivers does not increase monotonically with the fare rate of taxis (Fig. 9(f), which is the same for RSV drivers and RSV fare rate (Fig. 9 (k)). The reasons are

twofold. On the one hand, passengers can choose their hailing type with a lower fare rate. On the other hand, the hailing demand may shift to public transit due to higher hailing costs (Fig. 9(b) and (c)). Furthermore, an increase in lower taxi fare rates could make ridesourcing services more competitive and would increase profits for RSV drivers and the TNC. Nevertheless, RSV drivers and the TNC may also lose profits when taxi fare rate is overcharged (Fig. 9(j) and (n)), as hailing demand would be higher. Similarly, increasing the fare rate of RSVs can increase TNC's profit to an upper bound, but overpricing may lead to passenger losses, resulting in a decrease in TNC's profit (Fig. 9(o)). It should be noted that we did not model the labor supply of drivers, so the wage rate for RSV drivers only affects the profits of RSV drivers and the TNC.

Additionally, as the number of taxis and the wage rate for hybrid taxis may influence the market performance, we present a sensitivity analysis in Appendix D to examine the impact of these two key exogenous variables on different objectives.

5.3 Pareto optimal combined regulatory strategy

This section will validate the solution framework presented in Section 4.3 and analyze the optimal combined regulatory strategy. Based on the setting of the benchmark case $\boldsymbol{\varphi}_0 = [1400, 3.0, 2.5, 90\%]$, we further set the solution space Ω as follows:

$$\Omega = \begin{cases} 700 \le Z^{\text{rsv}} \le 2100 \\ 1.5 \le \alpha^{\text{taxi}} \le 4.5 \\ 1.5 \le \alpha^{\text{rsv}} \le 4.5 \\ 0.7 \le \tau^{\text{rsv}} < 1 \end{cases}, \tag{39}$$

where the upper and lower bounds of the domain for each decision variable are determined based on $\pm 50\%$ expansion of the benchmark value. Specifically, the domain of the RSV fare rate is set to be the same as that for the taxi fare rate. Meanwhile, the Chinese government also requires that the wage rate for RSV drivers cannot be lower than 70%.

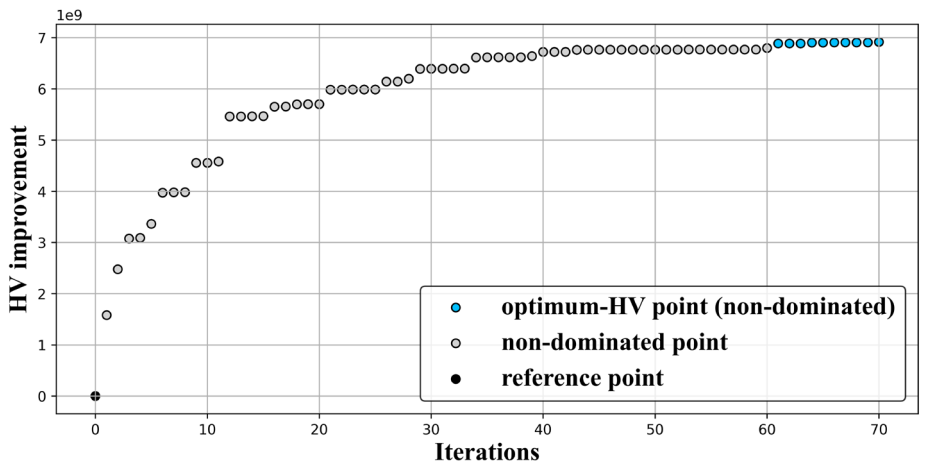

Fig. 10. Changes in the HV improvement over iterations.

Using 10 randomly selected points $\{\boldsymbol{\varphi}^1,\ldots,\boldsymbol{\varphi}^{10}\}$ from Ω and their corresponding objective values $\{\mathbf{f}(\boldsymbol{\varphi}^1),\ldots,\mathbf{f}(\boldsymbol{\varphi}^{10})\}$ as the initial samples of multi-objective Bayesian optimization, we obtained the HV improvement of the Pareto frontier over 70 iterations in Fig. 10, where objective values are computed using Algorithm B.3 during each iteration.

During each iteration of multi-objective Bayesian optimization, the acquisition function chooses a new sampling solution within Ω. In the first 21 iterations, the HV improvement value increases rapidly from 0 to nearly 6×10^9. This increase accounts for more than 85% of the global improvement. After the 60th iteration, updating the Pareto frontier no longer significantly increases the HV improvement value, and the Pareto frontier tends to be stabilized. It should be noted that the points acquired by the multi-objective Bayesian optimization within 70 iterations are all non-dominated.

The final output solution is selected according to the principle of maximum total vehicle utilization among the Pareto frontier, which is from the 66th iteration. Meanwhile, the last 10 solutions with the highest HV improvement values on the Pareto frontier are marked in blue for further analysis alongside the output solution. As illustrated in Fig. 11, the output solution $\boldsymbol{\varphi}^*$ contains 835 RSVs, with a taxi fare rate of 3.83 (¥/km), an RSV fare rate of 3.06 (¥/km), and a TNC wage rate for RSV drivers of 86%. This solution results in a total vehicle utilization rate of 84.25%.

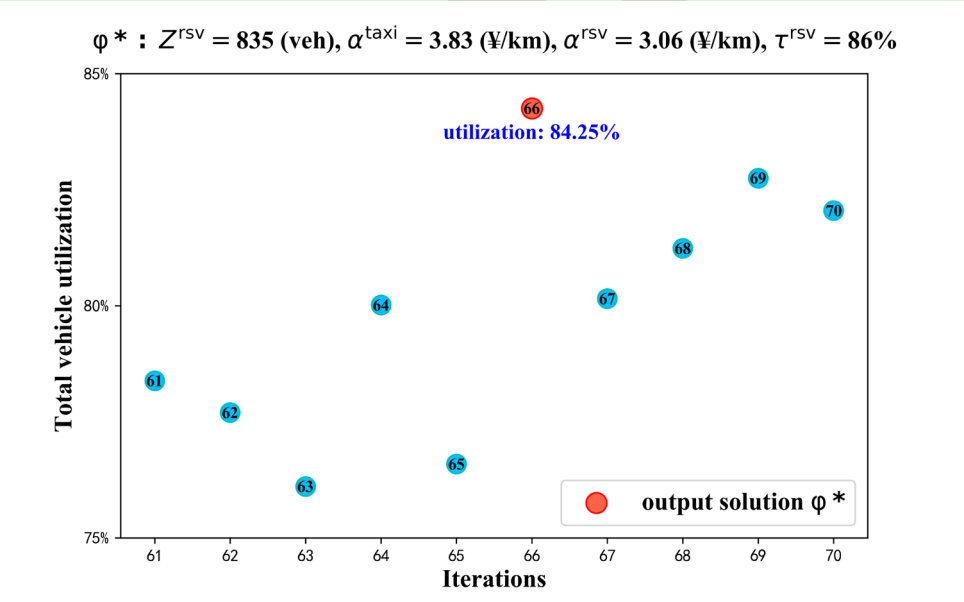

Fig. 11. Selection of the output solution based on maximizing total vehicle utilization.

Fig. 12 illustrates the distribution of objective values for these optimum-HV points and the benchmark case. In the output solution, fewer RSVs and higher fare rates for both hailing types reduce competition and increase incomes, making RSV and taxi drivers the most profitable stakeholders. Although the TNC can pay RSV drivers a lower wage rate and charge passengers a higher fare rate, the reduced number of RSVs only marginally increases its profit relative to the benchmark, while passengers incur higher hailing costs. From the Pareto perspective, shifting more hailing costs to

passengers appears to be unavoidable for improving market performance. Among the 10 selected optimum-HV points, only the 61st iteration resulted in a lower hailing cost than the benchmark case; however, both RSV drivers and the TNC lose profits, and taxi drivers' profits do not have a significant improvement. Note that in the Pareto frontier obtained from Fig. 10, the average passengers' hailing cost is 32.5 (¥), which is 12.5% (via $32.5/28.9-1$) more than the benchmark level.

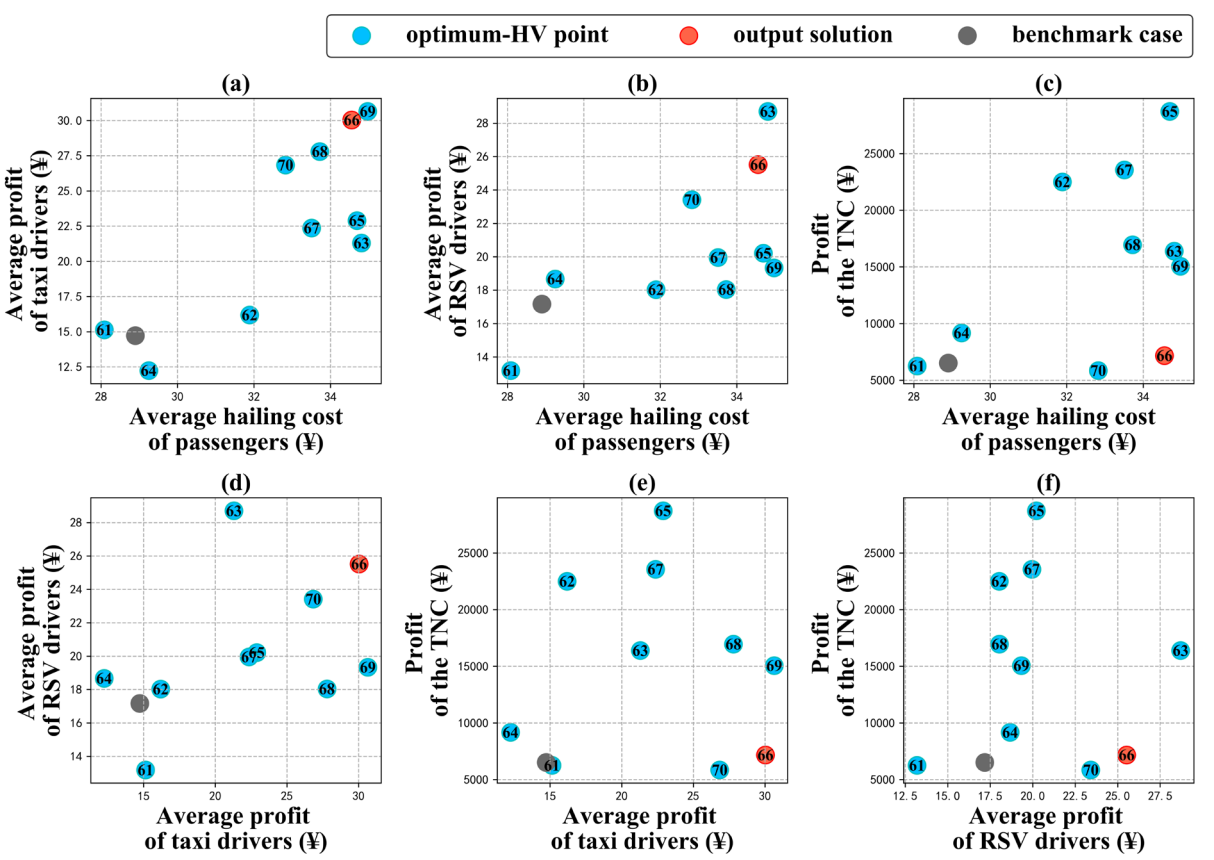

Fig. 12. The values of objective functions correspond to optimum-HV points, the output solution, and the benchmark case.

Table 3

Performance comparison of different combined regulatory strategies.

Solution type	Decision variable				Objective function				Total vehicle utilization
	Z^{rsv}	α^{taxi}	α^{rsv}	τ^{rsv}	$-\bar{C}$	Q^{taxi}	Q^{rsv}	Q^{TNC}	
Benchmark solution φ_0	1400	3.0	2.5	0.9	−28.9	14.7	17.2	6516	81.05%
Random solution 1	1868	2.78	2.15	0.99	−26.3	6.67	13.2	1274	75.74%
Random solution 2	1207	2.01	1.58	0.84	−24.7	4.0	2.7	5681	84.01%
Pareto optimal output solution φ^*	835	3.83	3.06	0. 86	**−34.6**	**30.0**	**25.5**	**7172**	**84.25%**

We select the benchmark solution and two randomly selected solutions to compare with the output solution (Table 3). We can see that the Pareto optimal output solution demonstrates significant advantages over the benchmark and random solutions, delivering enhanced welfare for taxi drivers, RSV drivers, and the TNC, alongside increased total vehicle utilization, while passengers are required to bear more hailing costs. Although the output solution cannot dominate all the objectives, the profits of taxi drivers, RSV drivers, and the TNC improved by 104.1%, 48.3%, and 10.1% compared to the benchmark, respectively, with 19.7% of the cost increase for passengers.

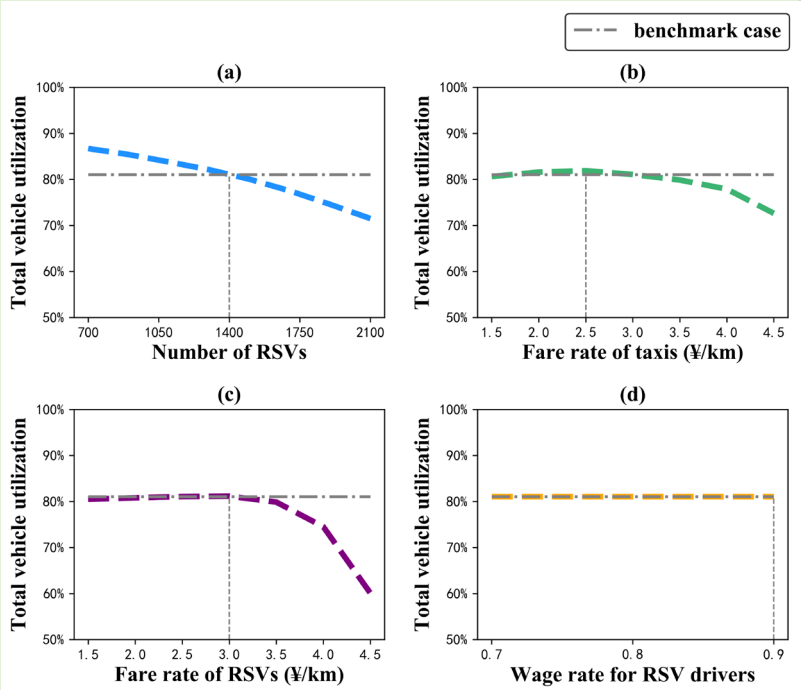

Fig. 13. Impact of four regulatory strategies on total vehicle utilization.

To figure out the relationship between the output solution and the total vehicle utilization, Fig. 13 illustrates the impact of the number of RSVs, the fare rates of taxis and RSVs, and the wage rate for RSV drivers on total vehicle utilization. Each subfigure is examined using Algorithm B.3 by varying a single decision variable while keeping the others fixed at the benchmark setting. It's clear that the number of RSVs results in an overall negative impact on total vehicle utilization, and higher fare rates would decrease utilization, while the impact of the RSV wage rate is found to be insignificant. Accordingly, if the output solution is selected at the Pareto frontier based on the principle of maximum total vehicle utilization, it's very likely to result in solutions with fewer RSVs and less expensive fare rates. However, a lower number of RSVs will negatively impact passengers and the TNC, while lower taxi and RSV fare rates will negatively impact the profits of taxi drivers, RSV drivers, and the TNC (Fig. 9 (f), (g), (j), (k), (n), (o)).

Besides, the government can select the appropriate solution on the Pareto frontier according to the market situation. Table 4 displays the benchmark case and four solutions in the set of non-dominated points that are most favorable to passengers, taxi drivers, RSV drivers, and the TNC, respectively. Obviously, every stakeholder could benefit compared to the benchmark case under

corresponding favorable regulation. If the government favors passengers, more RSVs and lower fare rates are needed. If the government favors taxi drivers, fewer RSVs and higher taxi fare rates are required. If the government favors RSV drivers, higher RSV fares and wage rates are needed. If the government favors the TNC, it requires more RSVs, higher fare rates, and pays RSV drivers the lowest wage rate. However, when the government prioritizes the passengers' welfare, both taxi and RSV drivers will lose profits, and the TNC's profit and the vehicle utilization are slightly lower than the benchmark level. Meanwhile, under a TNC-favored strategy, passengers bear higher hailing costs, yet neither taxi nor RSV drivers achieve significant profit gains, and the transportation system becomes inefficient, with total vehicle utilization approximately 10% lower than the benchmark (81.05% vs. 71.68%). Thus, prioritizing passenger welfare may not lead to driver-friendly regulation, whereas prioritizing the TNC's profit could be the worst option for government regulation, as it not only harms passengers but also substantially reduces total vehicle utilization.

Table 4

Pareto optimal results for different favorable stakeholders.

Beneficiary	Decision variable				Objective function				Total vehicle utilization
	Z^{rsv}	α^{taxi}	α^{rsv}	τ^{rsv}	$-\bar{C}$	Q^{taxi}	Q^{rsv}	Q^{TNC}	
None ($\boldsymbol{\varphi}_0$)	1400	3.0	2.5	0.9	−28.9	14.7	17.2	6516	81.05%
Passenger	1609	2.79	2.19	0.86	**−26.9**	10.1	10.7	6259	80.02%
Taxi	813	4.01	3.10	0.80	−35.3	**31.9**	22.9	9720	83.60%
RSV	1295	3.89	3.67	0.95	−35.0	26.8	**37.2**	4924	80.93%
TNC	1921	3.66	3.89	0.70	−34.7	15.4	17.7	**31492**	71.68%

5.4 Discussions

5.4.1 Optimizing the combined regulatory strategy from a single-objective perspective

In comparison to the prevailing literature that examined the regulation of the ridesourcing market based on a single objective, i.e., social welfare, this section establishes a single-objective function of social welfare and analyzes the corresponding optimal combined regulatory strategy. The social welfare of CRTM in a modeling time interval T is formulated as:

$$SW(\boldsymbol{\varphi}) = -w^{\text{pas}} \sum_{i=1}^{N\left(T,\lambda^*(\boldsymbol{\varphi})\right)} C_i + w^{\text{taxi}} Q^{\text{taxi}} Z^{\text{taxi}} + w^{\text{rsv}} Q^{\text{rsv}} Z^{\text{rsv}} + w^{\text{TNC}} Q^{\text{TNC}}, \tag{40}$$

where $SW(\boldsymbol{\varphi})$ is a function of $\boldsymbol{\varphi}$, note that its value could be negative since we use the average hailing cost to represent the welfare of passengers; w^s is the weight assigned to each stakeholder, $s \in \{\text{pas, taxi, rsv, TNC}\}$, $\sum w^s = 1$.

Based on the solution framework presented in Section 4.3, we calculate $SW(\boldsymbol{\varphi})$ using Algorithm B.3 in each iteration. The Expected Improvement (Jones et al., 1998; Mockus, 1998) is adopted as the acquisition function for single-objective Bayesian optimization. Table 5 shows the optimization results

under different government regulatory strategies with a certain prioritization, where we set w^s=0.7 to indicate a favored weight for a group $s \in$ {pas, taxi, rsv, TNC} .

Table 5

Optimal results (using social welfare) for different government regulatory focuses.

Beneficiary and weight $\mathbf{w}$	Decision variable				Objective function					Total vehicle utilization
	Z^{rsv}	α^{taxi}	α^{rsv}	τ^{rsv}	$SW(\boldsymbol{\varphi})$	$-\bar{C}$	Q^{taxi}	Q^{rsv}	Q^{TNC}	
Benchmark $\boldsymbol{\varphi}_0$	1400	3.0	2.5	0.9	/	−28.9	14.7	17.2	6516	81.05%
Evenhanded [0.25] * 4	820	4.5	4.5	0.75	−28658	−39.9	43.2	36.4	16574	84.97%
Passenger [**0.7**, 0.1, 0.1, 0.1]	1424	4.5	1.5	1.0	−95528	**−26.7**	4.8	5.0	769	69.50%
Taxi [0.1, **0.7**, 0.1, 0.1]	700	4.5	4.5	0.7	10135	−40.1	**44.4**	33.1	17329	85.93%
RSV [0.1, 0.1, **0.7**, 0.1]	2100	4.5	4.42	1.0	43245	−38.0	5.1	**45.6**	719	67.11%
TNC [0.1, 0.1, 0.1, **0.7**]	2100	4.5	4.5	0.7	10600	−38.2	13.2	25.0	**41283**	67.65%

Note $\mathbf{w} = [w^{\text{pas}}, w^{\text{taxi}}, w^{\text{rsv}}, w^{\text{TNC}}]$.

First, the results obtained by single-objective optimization have some similarities with those obtained by multi-objective optimization. If the government doesn't focus on a specific stakeholder (i.e., the Evenhanded solution in Table 5 and the Pareto output solution $\boldsymbol{\varphi}^*$ in Table 3), both solutions have fewer RSVs, higher fare rates, and lower RSV wage rates, as well as high vehicle utilizations. Meanwhile, the passenger-favored regulations may lead to a harmful market for both drivers and the TNC (Q^{taxi} = 4.8 and Q^{rsv} = 5.0 in Table 5), which is the same in multi-objective optimization. Moreover, both the TNC-favored regulations could not significantly improve drivers' profits and could lead to higher hailing costs for passengers (−34.7 in Table 4 and −38.2 in Table 5).

In this study, if the government prefers to regulate CRTM by maximizing social welfare, the RSV-favored solution is the best choice, which has the maximum $SW(\boldsymbol{\varphi})$ and a 165% (via $45.6/17.2 - 1$) improvement in the average profit of RSV drivers compared to the benchmark case. However, this regulation is impractical, as the profits of both taxi drivers and the TNC are very low, and the total vehicle utilization is 13.9% (via $81.05\% - 67.11\%$) lower than the benchmark level.

Additionally, since most solutions obtained in Table 5 are bound by the solution space Ω, an ensuing auxiliary experiment is to examine the single-objective optimization results under a larger solution space Ω', which is specified in Eq. (41). In this experiment, the objective weight w^s of each favored group s is also set to be 0.7. From the results presented in Table 6, it can be found that the optimal fare rates of RSV and taxi services increase except for the passenger-favored solution, since lower fare rates and more RSVs help reduce passengers' time and fare costs. Besides, the results show worse vehicle utilizations except for the taxi-favored solution, which is reasonable because this solution would lead to a minimum RSV cap to enhance the competitiveness of taxis. Based on Fig. 13(a), fewer RSVs generate higher vehicle utilization. Moreover, all the solutions are impractical

because some drivers would suffer losses from working. Specifically, taxi drivers would lose 18 ¥ in 30 minutes under the Evenhanded solution in Table 6. This could suggest that when regulating CRTM by a single objective of maximizing social welfare, the taxi industry may be removed from the market without special attention. Yu et al. (2020) also found that if the government did not place more weight on taxi drivers, it would be hard for them to survive in the market.

$$\Omega' = \begin{cases} 100 \le Z^{rsv} \le 3000 \\ 0.1 \le \alpha^{taxi} \le 10.0 \\ 0.1 \le \alpha^{rsv} \le 10.0 \\ 0.1 \le \tau^{rsv} < 1 \end{cases}. \tag{41}$$

Table 6

Optimal results of single-objective optimization with the larger solution space Ω'.

Beneficiary	Decision variable				Objective function					Total vehicle utilization
	Z^{rsv}	α^{taxi}	α^{rsv}	τ^{rsv}	$SW(\varphi)$	$-\bar{C}$	Q^{taxi}	Q^{rsv}	Q^{TNC}	
Evenhanded	1216	9.2	8.9	0.54	−23404	−64	−18	57	78543	55.21%
Passenger	2430	4.6	0.1	0.1	−67207	**−14**	−18	−19	3231	59.77%
Taxi	100	9.0	9.5	0.84	49433	−58	**120**	−17	3042	80.30%
RSV	2221	9.2	8.7	1.0	107821	−61	−22	**98**	10.9	54.91%
TNC	3000	10	6.8	0.1	104313	−50	−22	−11	**197625**	49.36%

5.4.2 Implications of overlooking passenger patience

Passengers' impatient behavior is a key factor influencing market performance and, consequently, the design of government regulation in the CRTM. In this subsection, we consider a hypothetical market with patient passengers, those who neither abandon nor cancel orders, and whose hailing-type choices are unaffected by sunk costs. With the same solution framework presented in Section 4.3, we obtain Pareto optimal solutions in Table 7 and compare the results considering passenger patience.

In such a patient market, passengers would not abandon requests due to long waiting times or cancel RSV orders upon encountering a vacant taxi. Compared with the impatient market, the government could set a lower RSV fleet cap to reduce drivers' competition and impose a higher government-guided RSV fare rate to benefit RSV drivers and the TNC. However, because taxis cannot 'steal' passengers already matched with RSVs, their profitability declines. To maintain taxi drivers' profits, the government would need to lower taxi fares to attract more hailing passengers. Furthermore, in the last row of Table 7, we show the values of four objective functions when implementing the patient regulatory strategies in the impatient market. It is found that only minor changes appear in the vehicle utilization and the welfare of passengers, RSV drivers, and the TNC, while taxi drivers lose 23.3% of profits (via $1 - 23.1/30.0$). We conclude that regulating the CRTM without accounting for passenger impatience may lead to underestimating taxi driver profitability and setting fares too low, thereby causing drivers to forgo potential profits.

Table 7

Pareto optimal solutions of impatient and patient passengers.

Market type	Decision variable				Objective function				Total vehicle utilization
	Z^{rsv}	α^{taxi}	α^{rsv}	τ^{rsv}	$-\bar{C}$	Q^{taxi}	Q^{rsv}	Q^{TNC}	
Impatient	835	3.83	3.06	0.86	−34.6	30.0	25.5	7172	84.25%
Patient	795	2.94	3.63	0.85	−33.8	21.2	31.0	7532	85.16%
Implement patient regulation in the impatient market					−34.4	23.1	28.7	7290	85.15%

6 Conclusion

Ridesourcing has improved travel services and efficiency for passengers, but the large influx of RSV drivers and the irrational operation of TNCs in recent years have posed great challenges to the government's regulatory work. This paper presents a multi-objective bi-level programming model to help policymakers find a Pareto optimal combined regulatory strategy for CRTM, including RSV fleet cap, taxi and RSV fare rate control, and TNC wage rate floor. The upper-level problem is to determine the combination of regulatory strategies with the objectives of minimizing the average hailing cost of passengers and maximizing the average profit of taxi drivers, the average profit of RSV drivers, and the profit of the TNC. The lower level aims to reflect the steady-state market performance under different regulations, where an agent-based simulation is developed to examine the impact of different regulatory strategies. The simulation model not only captures the travel mode choice and hailing type choice behaviors of passengers but also the work mode choice of taxi drivers between online matching and street cruising. Moreover, the abandonment and different cancellation behaviors of impatient passengers before and after order matching are considered. To solve the bi-level model, we developed a solution framework based on multi-objective Bayesian optimization, which can capture the complex nonlinear relationships in CRTM and substantially decrease calls to the lower-level simulation. During each iteration, the lower-level problem is solved as a fixed-point problem via iterating the agent-based simulation to obtain stabilized hailing demand and market supply. After validating the simulation model with a real-world dataset, experiments are conducted to illustrate the impact of the different regulatory strategies and explore the Pareto optimal solution for the government.

The main findings of this study can be summarized as follows:

(1) If the government regulates CRTM without considering the impatience of passengers, it may underestimate the profitability of taxi drivers and implement a lower taxi fare rate, causing taxi drivers to lose potential profits.

(2) No single strategy can simultaneously benefit passengers, taxi drivers, RSV drivers, and the TNC; excessively high fare rates instead reduce the profitability of both drivers and the TNC.

(3) When selecting a solution from the Pareto frontier coupled using a secondary criterion of maximizing total vehicle utilization, the government should set a lower RSV fleet cap than in the benchmark case, impose higher taxi and government-guided RSV fare rates, and allow the TNC to pay RSV drivers lower wage rates.

(4) Increasing passenger hailing costs appears to be an unavoidable trade-off for improving overall market performance. This increase could reach up to 12.5%.

(5) If the government prioritizes passengers in its regulation, both RSV and taxi drivers would lose profits. Under a TNC-favored regulation, passengers would face higher costs, while total vehicle utilization may become inefficient.

(6) If the government prefers to regulate CRTM in a single-objective manner by maximizing social welfare, it should lower the RSV fleet cap and increase hailing fare rates. While the RSV-favored regulation generates the highest social welfare, it is impractical to implement due to poor overall market performance.

Furthermore, this paper identifies several promising directions for future research, which can be categorized into two main areas. First, regarding the agent-based simulation of hailing services, future research could explore the impact of allowing drivers to cancel assignments when the pick-up location is far from their current position. Such cancellations might influence drivers' satisfaction, passengers' waiting time, and overall market efficiency (Zhang et al., 2023; Xu et al., 2024). Incorporating a more dynamic decision-making process for drivers in the model could yield deeper insights into the interplay between driver behaviors and market dynamics. Second, concerning CRTM regulation, the bi-level model and solution framework developed in this study demonstrate the capability to handle optimization problems with high-dimensional objective functions and decision variables. This flexibility provides opportunities to explore more complex government regulatory strategies and stakeholder interactions. For instance, while this paper focuses on a single TNC, future research could investigate market dynamics involving multiple competing TNCs and the corresponding regulatory challenges for governments (Guo et al., 2019; Siddiq and Taylor, 2022). Similarly, addressing the regulation of passengers who frequently cancel orders or those who simultaneously request services from multiple platforms warrants further investigation. If the time-resolved traffic data is available, it is also promising to investigate a time-dependent fleet cap over an extended modeling horizon.

Appendix A. The agent-based simulation framework

The following table lists the agents' states, behaviors, properties, and KPIs in the agent-based simulation framework. The states, behaviors, properties, and KPIs mentioned in our framework are not exhaustive but represent the focus of attention in this study.

Table A.1

Agent types, states, behaviors, properties, and KPIs

Types	States	Behaviors	Properties	KPIs
Passenger	● Waiting to be matched ● Abandoned ● Canceled before order matching ● Matched ● Canceled after order matching ● Served by an RSV ● Served by a hybrid taxi ● Served by a cruising taxi ● Served by public transit ● Left the system (completed hailing/transit trip)	● Travel mode choice (public transit or hailing service) ● Hailing type choice (RSV or taxi) ● Abandon request ● Cancel order (before or after order matching)	● ID ● Arrival time ● Origin and destination ● Maximum waiting time ● Time cost coefficient ● Sunk cost coefficient ● Psychological cost	● Waiting time ● Answer time ● Pick-up time ● Hailing cost
RSV	● Idle ● Picking up ● In-service	● Driving direction choice	● ID ● Current location ● Target location ● Current travel direction ● Time to become available ● Time cost coefficient ● Fuel cost coefficient ● Fixed operating cost	● Idling distance ● Pick-up distance ● Service distance ● Wasted distance ● Service volume ● Operating profit ● Vehicle utilization
Taxi	● Idle ● Picking up ● In-service	● Driving direction choice ● Work mode choice	● ID ● Current location ● Target location ● Current travel direction ● Time to become available ● Time cost coefficient ● Fuel cost coefficient ● Fixed operating cost	● Idling distance ● Pick-up distance ● Service distance ● Wasted distance ● Online service volume ● Cruising service volume ● Operating profit ● Vehicle utilization

Note: Vehicle utilization is the ratio of service distance to total distance driven.

Appendix B. Main loops of the simulation

Algorithm B.1 represents the basic agent-based simulation process of CRTM, which simulates the interactions and behaviors of drivers and passengers in the market and would be called multiple times by Algorithm B.2 and B.3. Algorithm B.2 is used in Section 5.1, its task is to stabilize drivers' work mode choices and their time cost coefficients under a given hailing demand rate and output corresponding market performance metrics. Algorithm B.3 represents the lower-level model of the research problem, which outputs market performance metrics with a stabilized supply-demand pattern under a given combined regulatory strategy. It is used in Sections 5.2-5.4.

Algorithm B.1: Basic simulation loop of CRTM within one time interval T.

Input: Combined regulatory strategy $\boldsymbol{\varphi}$, hailing demand λ, average profit of hybrid taxis $Q^{\text{h-taxi}}$ and street taxis $Q^{\text{s-taxi}}$, time cost coefficients of RSVs β^{rsv} and hybrid taxis $\beta^{\text{h-taxi}}$
Output: Market performance metrics

Set warm-up time $T_0 = 10\% \times T$, time stamp $ts = 1$
Generate passengers, RSVs, taxis, and initialize simulation settings
while time stamp $ts \le T + T_0$ **do**
    Update vehicles' locations and travel directions
    if number of unmatched passengers > 0 **&** number of available hailing vehicles > 0 **then**
        Match passengers with their preferred hailing vehicles based on the NN algorithm
    end if
    for passenger *i* who has arrived at t_i but hasn't been picked up **do**
        if passenger *i* hasn't been matched **then**
            if $ts - t_i > W_{\max}$ **then**
                Passenger *i* abandons the online request before order matching
            else if $ts - t_i \le W_{\max}$ & $u_i(ts - t_i) \ge \max\{\alpha^{\text{taxi}}, \alpha^{\text{rsv}}\}$ **then**
                Passenger *i* requests for both hailing types
            end if
            if the number of available hailing vehicles > 0 **then**
                Passenger *i* is matched
            else if no available hailing vehicles **&** encountering a vacant taxi **then**
                Passenger *i* cancels before order matching
            else
                Passenger *i* is waiting to be matched
            end if
        else if passenger *i* has been matched but hasn't been picked up **then**
            if $W_i^{\text{pick}} \le ts - t_i$ **then**
                Passenger *i* is picked up and served by an RSV or a hybrid taxi
            else if $W_i^{\text{pick}} > ts - t_i$ **&** encountering a vacant taxi **then**
                if $C_i^1 \le C_i^2$ **then**
                    Passenger *i* will keep waiting for the matched vehicle
                else
                    Passenger *i* cancels after order matching
                end if

else
Passenger i is waiting to be picked up
end if
end if
end for
if $ts > T_0$ **then**
Count and calculate market performance metrics
end if
end

Algorithm B.2: Simulation loop for stabilizing drivers' work mode split and time cost coefficients.

Input: Combined regulatory strategy $\boldsymbol{\varphi}$, hailing demand λ
Output: Average market performance metrics

Initialize $Q^{\text{h-taxi}}$, $Q^{\text{s-taxi}}$, β^{rsv}, $\beta^{\text{h-taxi}}$
Set $n=1$, $Z_0^{\text{h-taxi}}=0$, $Z_1^{\text{h-taxi}}=e^{\theta^{\text{taxi}}Q^{\text{h-taxi}}}\Big/\left(e^{\theta^{\text{taxi}}Q^{\text{h-taxi}}}+e^{\theta^{\text{taxi}}Q^{\text{s-taxi}}}\right)$
while $\left|Z_n^{\text{h-taxi}}-Z_{n-1}^{\text{h-taxi}}\right|<1$ (veh) **do**
$Z^{\text{s-taxi}} \leftarrow Z^{\text{taxi}}-Z_n^{\text{h-taxi}}$
Run $OneSim\left(\boldsymbol{\varphi},\lambda,\left[Q^{\text{h-taxi}},Q^{\text{s-taxi}},\beta^{\text{rsv}},\beta^{\text{h-taxi}}\right]\right)$ of Algorithm B.1 for 100 times and calculate the average market performance metrics
Update $Q^{\text{h-taxi}}$, $Q^{\text{s-taxi}}$, β^{rsv}, $\beta^{\text{h-taxi}}$
$Z_{n+1}^{\text{h-taxi}} \leftarrow e^{\theta^{\text{taxi}}Q^{\text{h-taxi}}}\Big/\left(e^{\theta^{\text{taxi}}Q^{\text{h-taxi}}}+e^{\theta^{\text{taxi}}Q^{\text{s-taxi}}}\right)$
$n \leftarrow n+1$
end

Algorithm B.3: Simulation loop for stabilizing supply-demand pattern.

Input: Combined regulatory strategy $\boldsymbol{\varphi}$
Output: Average market performance metrics

Initialize $\bar{L}$
Define a sequence of real numbers $\{\lambda_n\}$
Set $n=1$, $\lambda_0=0$, $\lambda_1=\Lambda e^{-\theta^{\text{pas}}\bar{L}}\Big/\left(e^{-\theta^{\text{pas}}\bar{L}}+e^{-\theta^{\text{pas}}\bar{C}^{\text{tansit}}}\right)$
while $\left|\lambda_n-\lambda_{n+1}\right|<1$ (request/min) **do**
$\lambda^{\text{transit}} \leftarrow \Lambda-\lambda_n$
Run $DriverStableSim\left(\boldsymbol{\varphi},\lambda_n\right)$ of **Algorithm B.2** and calculate the average market performance metrics
Calculate $\bar{C}^{\text{rsv}}$ and $\bar{C}^{\text{taxi}}$
$\bar{L}\left(\boldsymbol{\varphi},\lambda_n\right) \leftarrow \ln\left(e^{\theta_0\bar{C}^{\text{rsv}}}+e^{\theta_0\bar{C}^{\text{taxi}}}\right)\Big/\theta_0$
$\lambda_{n+1} \leftarrow \Lambda e^{-\theta^{\text{pas}}\bar{L}(\boldsymbol{\varphi},\lambda_n)}\Big/\left(e^{-\theta^{\text{pas}}\bar{L}(\boldsymbol{\varphi},\lambda_n)}+e^{-\theta^{\text{pas}}\bar{C}^{\text{tansit}}}\right)$
$n \leftarrow n+1$
end

Appendix C. Parameter settings

Table C.1

Parameter settings and corresponding sources/references.

Symbol	Value/Range	Unit	Source/Reference
Benchmark case φ_0			
Z^{rsv}	1400	(veh)	Average number of RSVs in the DiDi dataset between 7:00 to 23:00
α^{taxi}	3.0	(¥/km)	Market price in Hangzhou, 2018
α^{rsv}	2.5	(¥/km)	Market price in Hangzhou, 2018
τ^{rsv}	90	(%)	Market price in Hangzhou, 2018
Parameters / Exogenous variables			
T	30	(min)	Specified in this study
M	17	/	Estimated in Section 5.1
l_i	Between$[1,32]$	(km)	Calculated based on Eq. (5)
$\bar{l}$	≈11.3	(km)	Calculated based on Eq. (6)
R	5	(km)	Haliem et al. (2021); Manchella et al. (2021)
Λ	500	(requests/min)	Wang et al. (2020)
u_{max}	5	(¥/km)	Specified in this study
$\bar{C}^{transit}$	≈28.6	(¥)	Calculated based on Eq. (14)
$\bar{W}^{tansit}$	10	(min)	Beojone and Geroliminis (2021)
$\alpha^{transit}$	0.5	(¥/km)	Parameter setting of this paper
Z^{taxi}	814	(veh)	Estimated in Section 5.1
τ^{taxi}	0.95	(%)	Specified in this study
W_{max}	10	(min)	Beojone and Geroliminis (2021)
β^{pas}_{time}	1	(¥/min)	Wang et al. (2016); Li et al. (2022)
β^{pas}_{sunk}	0.1	(¥/km·min)	Specified in this study
$\hat{p}$	2	(¥)	Wang et al. (2020)
H	2	(¥)	Wang et al. (2020)
v,	0.5	(km/min)	BaiduMaps (2019)
v^{tansit}	$0.87\times v$=0.435	(km/min)	Kieu et al. (2015)
γ	0.5	(¥/km)	Xu et al. (2022)
$\hat{\gamma}^{rsv}, \hat{\gamma}^{taxi}$	10,15	(¥/30min)	Li et al. (2022)
$\theta^{pas}, \theta^{taxi}$	0.02,0.02	/	Wang et al. (2016)
θ_0	2	/	He et al. (2018)

Appendix D. Sensitivity analysis of the number and wage rate of taxis

Based on the basic assumptions in this study, the number of taxis Z^{taxi} and the wage rate for hybrid taxi drivers τ^{taxi} are exogenously given. However, these two exogenous variables might influence the system's performance. In Fig. D1, we examine the impact of the two factors on each objective function, where the results are computed under the benchmark case $\boldsymbol{\varphi}_0$ using Algorithm B.3. In brief, the results obtained are similar to those for RSV number and RSV wage rate (Fig. 9), where the impact of hybrid taxi wage rate on passengers and RSVs is both insignificant, and passengers and the TNC would benefit from more taxis, but drivers would not.

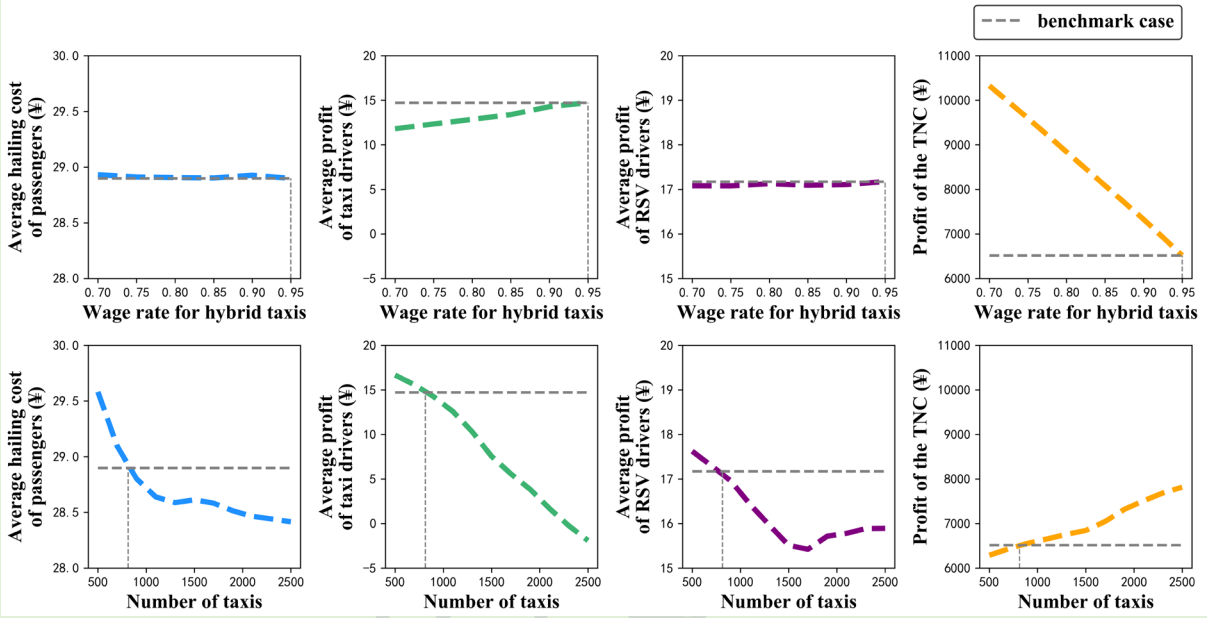

Fig. D1. Impact of taxi number and hybrid taxi wage rate on different objective functions.

References

Agatz, N., Erera, A.L., Savelsbergh, M.W.P., Wang, X., 2011. Dynamic ride-sharing: A simulation study in metro Atlanta. *Procedia-Social and Behavioral Sciences* 17, 532-550.

Bai, J., So, K.C., Tang, C.S., Chen, X., Wang, H., 2019. Coordinating supply and demand on an on-demand service platform with impatient customers. *Manufacturing & Service Operations Management* 21, 556-570.

BaiduMaps, 2019. 2018 Annual China City Transportation Report. Accessed: 8 July, 2025, https://renqi.map.baidu.com/reports/2018annualtrafficreport.html.

Banerjee, S., Riquelme, C., Johari, R., 2015. Pricing in ride-share platforms: A queueing-theoretic approach. *Available at SSRN 2568258*.

Ben-Akiva, M.E., Lerman, S.R., 1985. *Discrete choice analysis: theory and application to travel demand*. MIT press.

Beojone, C.V., Geroliminis, N., 2021. On the inefficiency of ride-sourcing services towards urban congestion. *Transp. Res. Part C Emerg. Technol.* 124, 102890.

Bertsimas, D.J., Van Ryzin, G., 1991. A stochastic and dynamic vehicle routing problem in the Euclidean plane. *Operations Research* 39, 601-615.

Besbes, O., Castro, F., Lobel, I., 2022. Spatial capacity planning. *Operations Research* 70, 1271-1291.

Beume, N., Naujoks, B., Emmerich, M., 2007. SMS-EMOA: Multi-objective selection based on dominated hypervolume. *Eur J Oper Res* 181, 1653-1669.

Campbell, H., 2023. Uber Statistics 2023: Drivers, Riders, Revenue, & More. The Rideshare Guy. https://therideshareguy.com/uber-statistics/#financial-performance-stats.

Castillo, J.C., Knoepfle, D., Weyl, G., 2017. Surge pricing solves the wild goose chase, *Proceedings of the 2017 ACM Conference on Economics and Computation*, pp. 241-242.

Chen, Z., Miao, Y., Ke, J., He, Q.-C., 2024. Operations and regulations for a ride-sourcing market with a mixed fleet of human drivers and autonomous vehicles. *Transp. Res. Part C Emerg. Technol.* 160, 104519.

Cheong, H.-i., Macias, J.J.E., Karamanis, R., Stettler, M., Majumdar, A., Angeloudis, P., 2023. Policy and Strategy Evaluation of Ridesharing Autonomous Vehicle Operation: A London Case Study. *Transportation Research Record*, 03611981231160157.

Clegg, J., Smith, M., Xiang, Y., Yarrow, R., 2001. Bilevel programming applied to optimising urban transportation. *Transp. Res. Part B Methodol.* 35, 41-70.

Couckuyt, I., Deschrijver, D., Dhaene, T., 2014. Fast calculation of multi-objective probability of improvement and expected improvement criteria for Pareto optimization. *Journal of Global Optimization* 60, 575-594.

Duong, H.L., Chu, J., Yao, D., 2023. Taxi drivers' response to cancellations and no-shows: New evidence for reference-dependent preferences. *Management Science* 69(1), 179-199.

Feng, G., Kong, G., Wang, Z., 2021. We are on the way: Analysis of on-demand ride-hailing systems. *Manufacturing & Service Operations Management* 23, 1237-1256.

Feng, S., Chen, T., Zhang, Y., Ke, J., Yang, H., 2023. A multi-functional simulation platform for on-demand ride service operations. *arXiv preprint arXiv:2303.12336*.

Feng, S., Ke, J., Xiao, F., Yang, H., 2022. Approximating a ride-sourcing system with block matching. *Transp. Res. Part C Emerg. Technol.* 145, 103920.

Flötteröd, G., 2017. A search acceleration method for optimization problems with transport simulation constraints. *Transp. Res. Part B Methodol.* 98, 239-260.

Frazier, P.I., 2018. Bayesian optimization, *Recent advances in optimization and modeling of contemporary problems*. Informs, pp. 255-278.

Gong, Y., Zhong, S., Zhao, S., Xiao, F., Wang, W., Jiang, Y., 2025. Optimizing green splits in high-dimensional traffic signal control with trust region Bayesian optimization. *Computer-Aided Civil and Infrastructure Engineering* 40(6), 741-763.

Guo, Y., Li, X., Zeng, X., 2019. Platform competition in the sharing economy: Understanding how ride-hailing services influence new car purchases. *Journal of Management Information Systems* 36, 1043-1070.

Haliem, M., Mani, G., Aggarwal, V., Bhargava, B., 2021. A distributed model-free ride-sharing approach for joint matching, pricing, and dispatching using deep reinforcement learning. *IEEE Transactions on Intelligent Transportation Systems* 22, 7931-7942.

Hamedmoghadam, H., Ramezani, M., Saberi, M., 2019. Revealing latent characteristics of mobility networks with coarse-graining. *Scientific reports* 9, 7545.

Han, J., Zhang, G., Hu, Y., Lu, J., 2016. A solution to bi/tri-level programming problems using particle swarm optimization. *Information Sciences* 370, 519-537.

He, F., Shen, Z.-J.M., 2015. Modeling taxi services with smartphone-based e-hailing applications. *Transp. Res. Part C Emerg. Technol.* 58, 93-106.

He, F., Wang, X., Lin, X., Tang, X., 2018. Pricing and penalty/compensation strategies of a taxi-hailing platform. *Transp. Res. Part C Emerg. Technol.* 86, 263-279.

Huo, J., Liu, C., Chen, J., Meng, Q., Wang, J., Liu, Z., 2023a. Simulation-based dynamic origin–destination matrix estimation on freeways: A Bayesian optimization approach. *Transportation Research Part E: Logistics and Transportation Review* 173, 103108.

Huo, J., Liu, Z., Chen, J., Cheng, Q., Meng, Q., 2023b. Bayesian optimization for congestion pricing problems: A general framework and its instability. *Transp. Res. Part B Methodol.* 169, 1-28.

Jiao, G., Ramezani, M., 2022. Incentivizing shared rides in e-hailing markets: Dynamic discounting. *Transp. Res. Part C Emerg. Technol.* 144, 103879.

Jiao, G., Ramezani, M., 2024. A real-time cooperation mechanism in duopoly e-hailing markets. *Transp. Res. Part C Emerg. Technol.* 162, 104598.

Jiao, G., Ramezani, M., 2025. On the inefficiencies in the multi-platform e-hailing market with impatient customers. *Transp. Res. Part C Emerg. Technol.* 178, 105153.

Jones, D.R., Schonlau, M., Welch, W.J., 1998. Efficient global optimization of expensive black-box functions. *Journal of Global optimization* 13, 455-492.

Karamanis, R., Anastasiadis, E., Stettler, M., Angeloudis, P., 2021. Vehicle redistribution in ride-sourcing markets using convex minimum cost flows. *IEEE Transactions on Intelligent Transportation Systems* 23, 10287-10298.

Ke, J., Li, X., Yang, H., Yin, Y., 2021. Pareto-efficient solutions and regulations of congested ride-sourcing markets with heterogeneous demand and supply. *Transportation Research Part E: Logistics and Transportation Review* 154, 102483.

Ke, J., Yang, H., Li, X., Wang, H., Ye, J., 2020. Pricing and equilibrium in on-demand ride-pooling markets. *Transp. Res. Part B Methodol.* 139, 411-431.

Li, B., Szeto, W., Zou, L., 2022. Optimal fare and fleet size regulation in a taxi/ride-sourcing market with congestion effects, emission externalities, and gasoline/electric vehicles. *Transportation Research Part A: Policy and Practice* 157, 215-243.

Li, M., Jiang, G., Lo, H.K., 2023a. Optimal cancellation penalty for competing ride-sourcing platforms under waiting time uncertainty. *Transportation Research Part E: Logistics and Transportation Review* 174, 103107.

Li, S., Tavafoghi, H., Poolla, K., Varaiya, P., 2019. Regulating TNCs: Should Uber and Lyft set their own rules? *Transp. Res. Part B Methodol.* 129, 193-225.

Li, W., Zhao, S., Ma, J., Nielsen, O.A., Jiang, Y., 2023b. Book-ahead ride-hailing trip and its determinants: Findings from large-scale trip records in China. *Transportation Research Part A: Policy and Practice* 178, 103875.

Liu, A., Zhong, S., Sun, D., Gong, Y., Fan, M., Song, Y., 2024a. Joint optimal pricing strategy of shared autonomous vehicles and road congestion pricing: A regional accessibility perspective. *Cities* 146, 104742.

Liu, X., Yang, H., Xiao, F., 2022a. Equilibrium in taxi and ride-sourcing service considering the use of e-hailing application. *Transportmetrica A: Transport Science* 18, 659-675.

Liu, Y., Feng, S., Bao, Y., Yang, H., 2025. Learning the on-demand adaptable matching range with a reinforcement learning. *Transp. Res. Part C Emerg. Technol.* 172, 105018.

Liu, Y., QI, J., Yang, H., Tang, Y., 2024b. The passenger waiting behavior with sunk waiting time: an empirical study in ride-sourcing market. *Available at SSRN 4285203*.

Liu, Z., Lyu, C., Huo, J., Wang, S., Chen, J., 2022b. Gaussian process regression for transportation system estimation and prediction problems: the Deformation and a Hat Kernel. *IEEE Transactions on Intelligent Transportation Systems* 23, 22331-22342.

Maister, D.H., 1984. *The psychology of waiting lines*. Harvard Business School Boston.

Manchella, K., Haliem, M., Aggarwal, V., Bhargava, B., 2021. Passgoodpool: Joint passengers and goods fleet management with reinforcement learning aided pricing, matching, and route planning. *IEEE Transactions on Intelligent Transportation Systems* 23, 3866-3877.

Martinez, L.M., Correia, G.H.A., Viegas, J.M., 2015. An agent-based simulation model to assess the impacts of introducing a shared-taxi system: an application to Lisbon (Portugal). *Journal of Advanced Transportation* 49, 475-495.

Mo, D., Wang, H., Cai, Z., Szeto, W., Chen, X.M., 2024. Modeling and regulating a ride-sourcing market integrated with vehicle rental services. *Transportation Research Part E: Logistics and Transportation Review* 192, 103797.

Mockus, J., 1998. The application of Bayesian methods for seeking the extremum. *Towards global optimization* 2, 117.

Ni, L., Chen, C., Wang, X.C., Chen, X.M., 2021. Modeling network equilibrium of competitive ride-sourcing market with heterogeneous transportation network companies. *Transp. Res. Part C Emerg. Technol.* 130, 103277.

Nie, Y.M., 2017. How can the taxi industry survive the tide of ridesourcing? Evidence from Shenzhen, China. *Transp. Res. Part C Emerg. Technol.* 79, 242-256.

Nourinejad, M., Ramezani, M., 2020. Ride-Sourcing modeling and pricing in non-equilibrium two-sided markets. *Transp. Res. Part B Methodol.* 132, 340-357.

Olofsson, S., Mehrian, M., Calandra, R., Geris, L., Deisenroth, M.P., Misener, R., 2018. Bayesian multi-objective optimisation with mixed analytical and black-box functions: Application to tissue engineering. *IEEE Transactions on Biomedical Engineering* 66, 727-739.

Osorio, C., 2019. High-dimensional offline origin-destination (OD) demand calibration for stochastic traffic simulators of large-scale road networks. *Transp. Res. Part B Methodol.* 124, 18-43.

Qi, H., & Li, Z., 2020. Putting precarity back to production: a case study of Didi Kuaiche drivers in the city of Nanjing, China. *Review of Radical Political Economics*, *52*(3), 506-522.

Qin, X., Ke, J., Yang, H., 2025. Government regulations for ride-sourcing services as substitute or complement to public transit. *Transport Policy*, 103776.

Ramezani, M., Valadkhani, A.H., 2023. Dynamic ride-sourcing systems for city-scale networks-Part I: Matching design and model formulation and validation. *Transp. Res. Part C Emerg. Technol.* 152, 104158.

Rasmussen, C.E., 2003. Gaussian processes in machine learning, *Summer school on machine learning*. Springer, pp. 63-71.

Rayle, L., Dai, D., Chan, N., Cervero, R., Shaheen, S., 2016. Just a better taxi? A survey-based comparison of taxis, transit, and ridesourcing services in San Francisco. *Transport Policy* 45, 168-178.

Santos, M.J., Curcio, E., Amorim, P., Carvalho, M., Marques, A., 2021. A bilevel approach for the collaborative transportation planning problem. *International Journal of Production Economics* 233, 108004.

Shapiro, A., 2018. New York City just voted to cap Uber and Lyft vehicles, and that could make rides more expensive. CNBC. https://www.cnbc.com/2018/08/08/new-york-city-votes-to-cap-uber-and-lyft-vehicles.html.

Siddiq, A., Taylor, T.A., 2022. Ride-hailing platforms: Competition and autonomous vehicles. *Manufacturing & Service Operations Management* 24, 1511-1528.

Sun, L., Teunter, R.H., Hua, G., Wu, T., 2020. Taxi-hailing platforms: Inform or Assign drivers? *Transp.*

Res. Part B Methodol. 142, 197-212.

Tang, W., Xie, N., Mo, D., Cai, Z., Lee, D.-H., Chen, X.M., 2023. Optimizing subsidy strategies of the ride-sourcing platform under government regulation. *Transportation Research Part E: Logistics and Transportation Review* 173, 103112.

Thaler, R.H., 1980. Toward a positive theory of consumer choice. *Journal of economic behavior & organization* 1(1), 39-60.

Thaler, R.H., 1985. Mental accounting and consumer choice. *Marketing science* 4(3), 199-214.

Thaler, R.H., 1990. Anomalies: Saving, fungibility, and mental accounts. *Journal of economic perspectives* 4(1), 193-205.

Thaler, R.H., 1999. Mental accounting matters. *Journal of Behavioral decision making* 12(3), 183-206.

Ülkü, S., Hydock, C., Cui, S., 2020. Making the wait worthwhile: Experiments on the effect of queueing on consumption. *Management Science* 66, 1149-1171.

Vignon, D., Yin, Y., Ke, J., 2023. Regulating the ride-hailing market in the age of uberization. *Transportation research part E: logistics and transportation review* 169, 102969.

Wang, G., Zhang, H., Zhang, J., 2024. On-demand ride-matching in a spatial model with abandonment and cancellation. *Operations Research* 72, 1278-1297.

Wang, H., Yang, H., 2019. Ridesourcing systems: A framework and review. *Transp. Res. Part B Methodol.* 129, 122-155.

Wang, X., He, F., Yang, H., Gao, H.O., 2016. Pricing strategies for a taxi-hailing platform. *Transportation Research Part E: Logistics and Transportation Review* 93, 212-231.

Wang, X., Liu, W., Yang, H., Wang, D., Ye, J., 2020. Customer behavioural modelling of order cancellation in coupled ride-sourcing and taxi markets. *Transp. Res. Part B Methodol.* 132, 358-378.

Wei, B., Sun, D.J., 2018. A two-layer network dynamic congestion pricing based on macroscopic fundamental diagram. *Journal of Advanced Transportation* 2018.

Wei, S., Feng, S., Ke, J., Yang, H., 2022. Calibration and validation of matching functions for ride-sourcing markets. *Communications in Transportation Research* 2, 100058.

Wen, J., Chen, Y.X., Nassir, N., Zhao, J., 2018. Transit-oriented autonomous vehicle operation with integrated demand-supply interaction. *Transp. Res. Part C Emerg. Technol.* 97, 216-234.

Xu, K., Saberi, M., Liu, T.-L., Liu, W., 2024. Economic analysis of ridesourcing markets considering driver order cancellation and platform subsidy. *Travel Behaviour and Society* 36, 100795.

Xu, K., Saberi, M., Liu, W., 2022. Dynamic pricing and penalty strategies in a coupled market with ridesourcing service and taxi considering time-dependent order cancellation behaviour. *Transp. Res. Part C Emerg. Technol.* 138, 103621.

Xu, X., Yan, N., Tong, T., 2021a. Longer waiting, more cancellation? Empirical evidence from an on-demand service platform. *Journal of Business Research* 126, 162-169.

Xu, Z., Chen, Z., Yin, Y., Ye, J., 2021b. Equilibrium analysis of urban traffic networks with ride-sourcing services. *Transportation science* 55, 1260-1279.

Yang, H., Leung, C.W.Y., Wong, S.C., Bell, M.G.H., 2010. Equilibria of bilateral taxi–customer searching and meeting on networks. *Transp. Res. Part B Methodol.* 44, 1067-1083.

Yang, J., Levin, M.W., Hu, L., Li, H., Jiang, Y., 2023. Fleet sizing and charging infrastructure design for electric autonomous mobility-on-demand systems with endogenous congestion and limited link space. *Transp. Res. Part C Emerg. Technol.* 152, 104172.

Yang, J., Zhao, D., Wang, Z., Jiang, W., 2021. Comprehending the Pricing Decision of Online Car-Hailing Services in China: Price Regulation Vs Entry Limitation, *Modern Management based on Big Data II and Machine Learning and Intelligent Systems III*. IOS Press, pp. 195-204.

Yao, R., Bekhor, S., 2024. A ridesharing simulation model that considers dynamic supply-demand interactions. *Journal of Intelligent Transportation Systems* 28, 31-53.

Yu, J.J., Tang, C.S., Max Shen, Z.-J., Chen, X.M., 2020. A balancing act of regulating on-demand ride services. *Management Science* 66, 2975-2992.

Zha, L., Yin, Y., Du, Y., 2018a. Surge pricing and labor supply in the ride-sourcing market. *Transp. Res. Part B Methodol.* 117, 708-722.

Zha, L., Yin, Y., Xu, Z., 2018b. Geometric matching and spatial pricing in ride-sourcing markets. *Transp. Res. Part C Emerg. Technol.* 92, 58-75.

Zha, L., Yin, Y., Yang, H., 2016. Economic analysis of ride-sourcing markets. *Transp. Res. Part C Emerg. Technol.* 71, 249-266.

Zhang, W., He, R., Chen, Y., 2023. Modelling and simulation of cancelling orders behaviour by driver and passenger on the ride-hailing platform. *International Journal of Intelligent Systems Technologies and Applications* 21, 153-175.

Zhong, S., Gong, Y., Zhou, Z., Cheng, R., Xiao, F., 2021. Active learning for multi-objective optimal road congestion pricing considering negative land use effect. *Transp. Res. Part C Emerg. Technol.* 125, 103002.

Zhong, Y., Yang, T., Cao, B., Cheng, T.C.E., 2022. On-demand ride-hailing platforms in competition with the taxi industry: Pricing strategies and government supervision. *International Journal of Production Economics* 243, 108301.